Application of the CRUEX++ methodology

Three case studies

Contents

1 Introduction

1.1 Choice of the case study catchments

The application of the CRUEX++ methodology is demonstrated on three case studies. In order to cover different catchment characteristics, the three basins have been identified according to their geographical situation, glacier cover and area.

The geographical situation has a high impact on the meteorological conditions. That is the reason why the Swiss PMP maps have been developed for three different wind sectors, i.e. north, south and west-north-west. The selection of the catchments should allow to consider PMP maps from different sectors.

In addition, in a country like Switzerland, where topography has a major influence on the hydrological processes, the presence of glaciers highly impacts on the discharge generation. The choice of the study catchments should therefore also account for the glacier cover.

Regarding the area of the catchment, it plays an important role because the magnitude of floods do not increase linearly with the size of the catchments. The discharge of floods of the same order of magnitude logarithmically increase with the surface. This aspect has been considered to determine the upper catchment surface of 230 km^2 beyond which the Swiss PMP maps should not be used in order to avoid unrealistic overestimations of the PMF.

The choice of three basins is certainly a compromise and does not represent an exhaustive list of catchments covering all possible combinations of the three above mentioned factors, but it has been assumed to be reasonably representative to prove the applicability of the methodology to different alpine catchments with different characteristics.

The chosen catchments are the basins of the Limmernboden dam (17.8 km^2), the Mattmark dam (38 km^2) and the Contra dam (233 km^2). Their geographical situation is shown on the map of Figure 1.1. The safety flood estimation is undertaken by applying the CRUEX++ methodology. It should be mentioned that the area of the Contra dam catchment is slightly outside of the application limits of the methodology. Nevertheless, the methodology has been applied in order to further exploit the limits of the methodology applied close to the transition zone, to which a great uncertainty could be attributed.

Finally, the results are presented and discussed for each catchment. The estimation of the return period of the safety flood using upper bounded statistical distributions has been compared to conventional statistical approaches, like AM (annual maxima) and POT (peak over threshold).

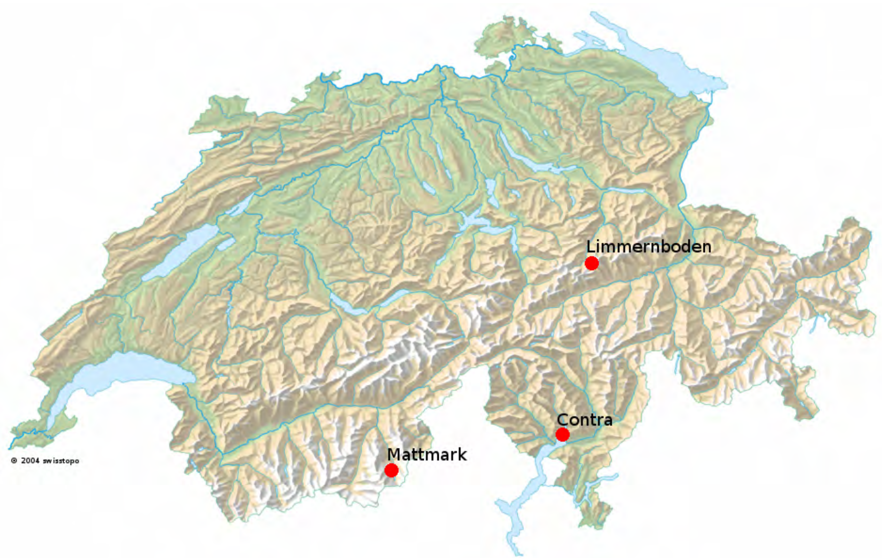

Figure 1.1: Situation of the three chosen case study dams in Switzerland.

1.2 Procedure for the application of the CRUEX++ methodology

The approach adopted for the application is exposed hereafter. For each of the three catchments, the following steps have been carried out.

1.2.1 Step 1: Catchment characteristics

First the catchment is characterised. The description of the catchments and the available data are important elements of the case study. It allows to expose the technical context of the study.

1.2.2 Step 2: The hydrological model

The second step is the hydrological model construction. The semi-distributed conceptual GSM-Socont model (Schaefli et al., 2005; Jordan et al., 2012; Schaefli and Zehe, 2009) has been used. The model takes into account the elevation of the catchment through altitude bands, in this case, with a vertical resolution of 300 m. The altitude bands have been determined based on a numerical terrain model with a horizontal resolution of 25 m. If lateral intakes are existing, the capacity of the collector has been estimated and considered in the model.

1.2.3 Step 3: Meteorological and discharge data

The model has then been calibrated and validated on observed data. The different considered meteorological stations have been exposed for each case study and the period of available data has been highlighted. The calibration and validation of the model has been done by comparing the simulated time series with the observed discharge time series made accessible by the dam operator. In the case of the Contra dam, two additional stations of the Federal Office for the Environment (FOEN) could be taken into account. The discharge data from the dam operators have been obtained by converting the level measurements into daily inflow volumes. Consequently, the discharge data are daily averaged values. Therefore, the model has to be assumed valid for smaller time steps when it is applied for flood estimations with intra-daily time resolution.

1.2.4 Step 4: Level-volume and level-outflow relations

The level-volume as well as the level-outflow relations of the reservoirs and spillways have been supplied by the dam operators for the Limmernboden and Mattmark dams. For the Contra dam, the level-outflow relation has been estimated. These relations have been implemented in the model to account for the flood attenuation and to evaluate the maximum level that occurred during the critical PMP event. The simulated maximum reservoir level and the corresponding outflow has than been used to verify if the existing spillway has been designed in order to make the dam withstand the safety flood event.

1.2.5 Step 5: PMP data

The PMP has been extracted from the Swiss PMP maps. The data of the PMP maps can be plotted as IDF curves (Intensity Duration Frequency) to derive PMP volumes for different event durations with an hourly time step has been performed. The PMP data have been temporally distributed using the 5% quantile rainfall mass curve provided in the methodology description. The temperature attributed to each PMP event has been derived from the linear relations between the precipitation duration and the maximum measured 0°C isothermal altitude, also reported in the methodology description.

1.2.6 Step 6: PMP-PMF simulation

The generation of the PMF event has been based on two different approaches. The first approach accounts deterministically for the initial conditions set for the PMP-PMF simulation. The longest possible simulation has been performed to generate state variable time series to derive the 99%

quantile values for a severe initialization of the model. The second approach uses a stochastic initial conditions scenario generator in order to account for the dependence between the different state variables. The two approaches have been compared in order to judge if the state variable dependences are representative or can be neglected. The here performed PMF estimation is used to determine the upper bound for the bounded statistical extrapolation carried out in a later step.

Due to the high impact of the initial conditions on the simulated discharge, a large number of different extreme floods can be obtained from a PMP event. For this study, median values for the initial state variable values have been admitted as terrain conditions for the estimation of the safety flood. If significant state variable dependences would lead to a big difference between the stochastically determined median safety flood discharge and the discharge derived under median initial conditions, the stochastic approach should be preferred. The PMP duration leading to the highest reservoir water level has been considered to generate the critical safety flood.

1.2.7 Step 7: Statistical distribution fit and estimation of the return period

The observed discharge data are daily averaged inflows. Daily flood estimates are, however, not valuable for the flood estimation in the context of dam safety verifications. Therefore, the calibrated hydrological model has been used to determine the maximum hourly inflow discharge data. This approach can extend the discharge time series when the meteorological time series is longer than the observed discharge series. The flood simulations (PMF and safety flood) have been performed with a 10 minutes time step. This short time step allowed to properly estimate the flood damping effect of the reservoir. However, this does not correspond to the time step of the extrapolated data set (hourly values derived by simulation). Therefore, a moving average approach has been used to determine the maximum hourly averaged discharge peak. The maximum hourly averaged PMF value has been retained as upper bound for the extrapolations. The upper bounded statistical distributions have been used to attribute a return period to the maximum hourly averaged safety flood.

Finally, a comparison of the extrapolations using upper bounded statistic distributions with the extrapolation from conventional distributions has been performed and discussed. The distributions that have been considered besides the EV4 and LN4, are the GEV (General Extreme Value distribution) and the Log-Normal distribution, as they are the parent distributions of the used bounded distributions. Furthermore, the POT method has been applied. It should be remembered that the application of the POT method refers to the fit of a two parameter GP (General Pareto) distribution. Its mathematical expression is provided in Appendix A.1. These three distributions (GEV, log-normal and GP) are commonly used in hydrology and are thus interesting to compare to the bounded distributions. The comparison allows to evaluate the benefits of the CRUEX++ methodology compared to the more traditional approaches.

2 Case studies

2.1 Application to the Limmernboden dam catchment

2.1.1 Description of the Limmernboden dam catchment

The Limmernboden concrete dam (Figure 2.1) is located in the northern part of the Swiss Alps in the canton of Glarus (Figure 1.1).

Figure 2.1: Photo of the Limmernboden dam (SwissCOD, 2011).

A detailed representation of the main catchment, the glacier cover, the reservoir and the lateral intakes are shown in Figure 2.2. The altitude range of the main catchment varies from 1 857 m.a.s.l. at reservoir level up to 3 419 m.a.s.l. and from 1 927 m.a.s.l. up to 3 614 m.a.s.l. for the lateral catchments. The total capacity of the lateral intakes is limited to 10.5 m^3/s. The main characteristics of the Limmernboden dam catchment, the reservoir and the lateral catchments are presented in Table 2.1.

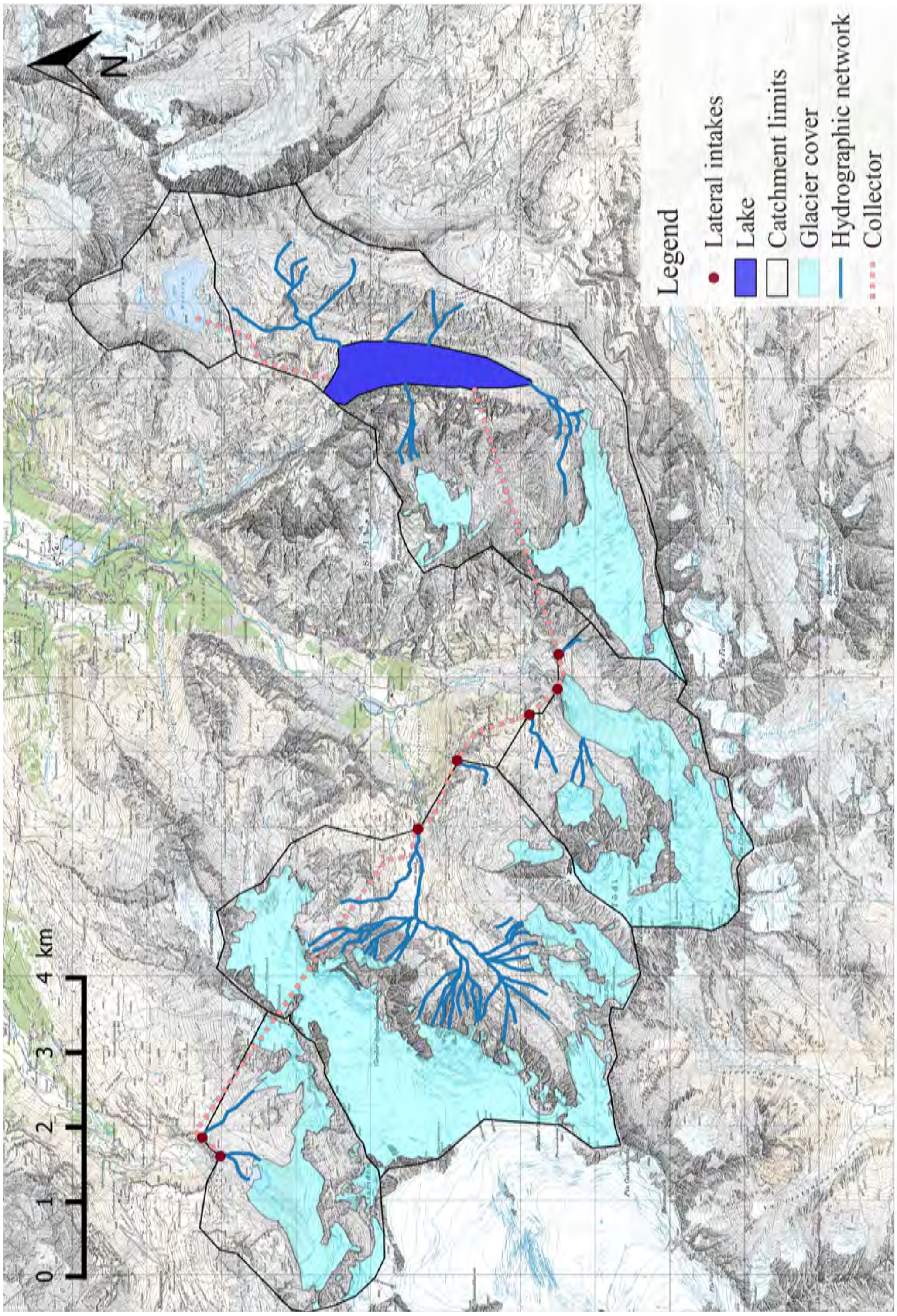

Figure 2.2: Limmernboden catchment with lateral catchments, glacier covered zones and the location of the intakes. Map source: Swisstopo

Table 2.1: Main characteristics of the Limmernboden catchment and the reservoir (SwissCOD, 2011)

Reservoir	
Name	Limmernboden
Canton	Glarus
Reservoir surface [km^2]	1.36
Volume [mio m^3]	92
Max spillway discharge [m^3/s]	89
Max discharge of ground outlet [m^3/s]	98
Spillway crest [m a.s.l.]	1857
Dam crest [m a.s.l.]	1858.5
Catchments	
Area [km^2]	17.8
Glacier cover [km^2]	2.2
Primary Inflows	Muttenbach
Primary Outflows	Limmernbach
External catchments	
Number of additional catchments	4
Additional area [km^2]	31.8
Additional glacier cover [km^2]	14.6
Collector capacity [m^3/s]	10.5

2.1.2 Description of the spillway of the Limmernboden dam

The spillway of the Limmernboden dam has been designed as lateral weir, situated on the left bank of the dam. The evacuated flow is then led into a gallery. According to the report on the hydraulic design of the spillway (KLL, 1988), this gallery could be damaged if it gets pressurized. Therefore its capacity should be high enough in order to evacuate the safety flood without pressurization. The spillway capacity is limited due to the latter criterion and has been estimated to be $Q = 90\,\mathrm{m^3/s}$ (KLL, 1988). Figure 2.3, taken from the report on the hydraulic design of the spillway (KLL, 1988), shows the situation of the Limmernboden dam with the lateral spillway and the gallery. In the same report, a profile of the spillway crest could be found. It is illustrated in Figure 2.4.

The level-outflow relation given in the report on the hydraulic design of the spillway (KLL, 1988) is plotted together with the level-volume relation in Figure 2.5.

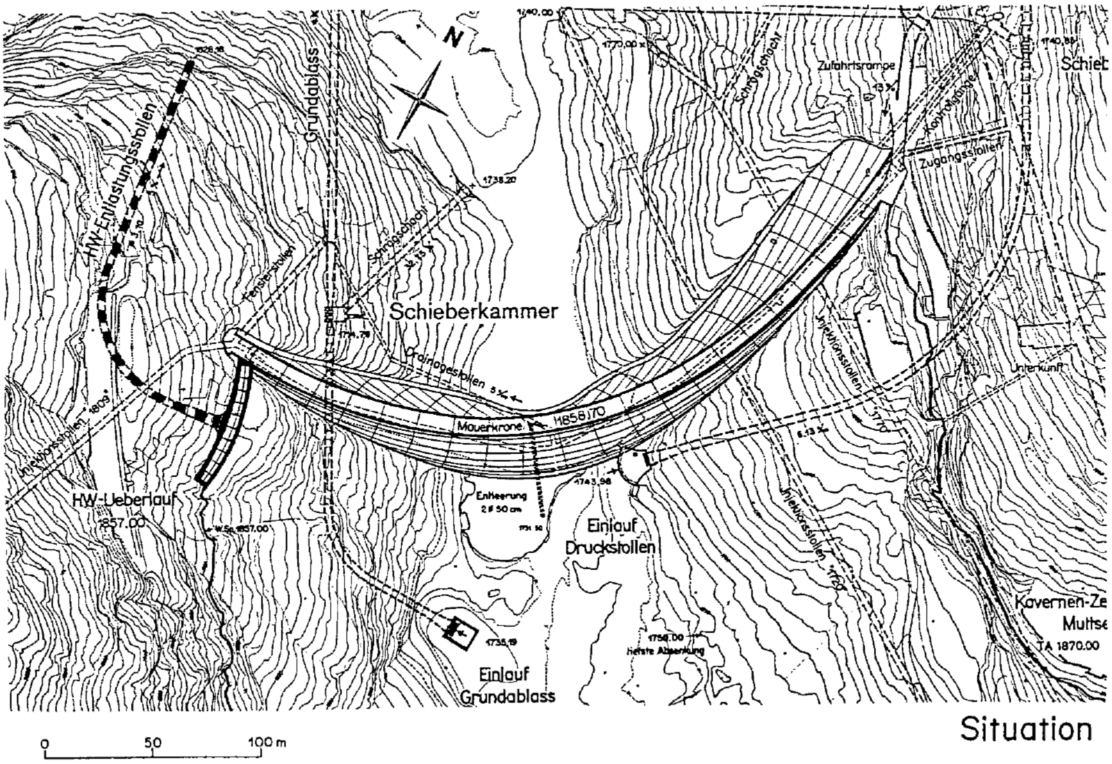

Figure 2.3: Limmernboden dam situation plan. Taken from the report on the hydraulic design of the spillway (KLL, 1988).

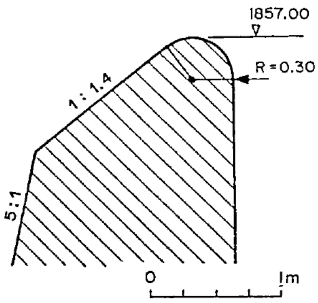

Figure 2.4: Limmernboden dam spillway crest profile. Taken from the report on the hydraulic design of the spillway (KLL, 1988).

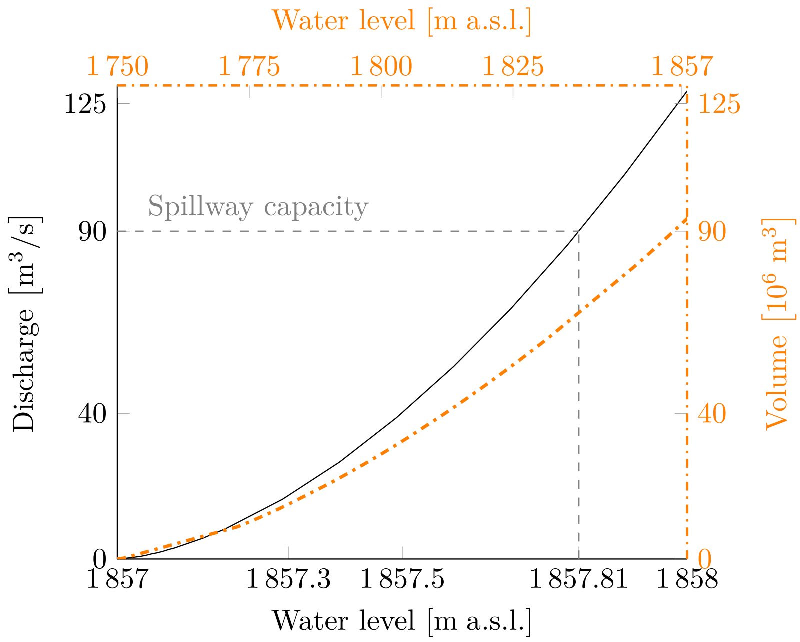

Figure 2.5: Spillway routing curve of the Limmernboden dam and level-volume relation of the reservoir.

2.1.3 Meteorological and discharge data

The available meteorological (precipitation and temperature) and discharge time series are briefly described in the following.

The situation of the meteorological stations around the Limmernboden dam catchment is illustrated in Figure 2.6. The meteorological data has been provided by MeteoSwiss. For the present analysis, 10 meteorological stations have been taken into account. At all stations precipitation data have been available but only at 4 stations temperature was measured for the period from 01/01/1981 to 31/12/2009.

Regarding the temporal resolution of the meteorological data sets, values at a daily time step have been available at the stations measuring only precipitation (cf Figure 2.6). For the stations measuring precipitation and temperature, data at an hourly time step was accessible. The daily data have been disaggregated in hourly data sets. To do so, two nearby stations, for which hourly data were available, had to be chosen. The data of these two stations were then interpolated, using the inverse squared distance weighting, to get an estimate of hourly precipitation at the location of the station to be disaggregated. Finally, the daily measured precipitation volume of the station to be disaggregated was used to adjust the volume of the generated hourly time series.

Figure A.2 illustrates the periods covered by the meteorological time series. The detailed dates of the begin and end of the time series are shown in Table A.1.

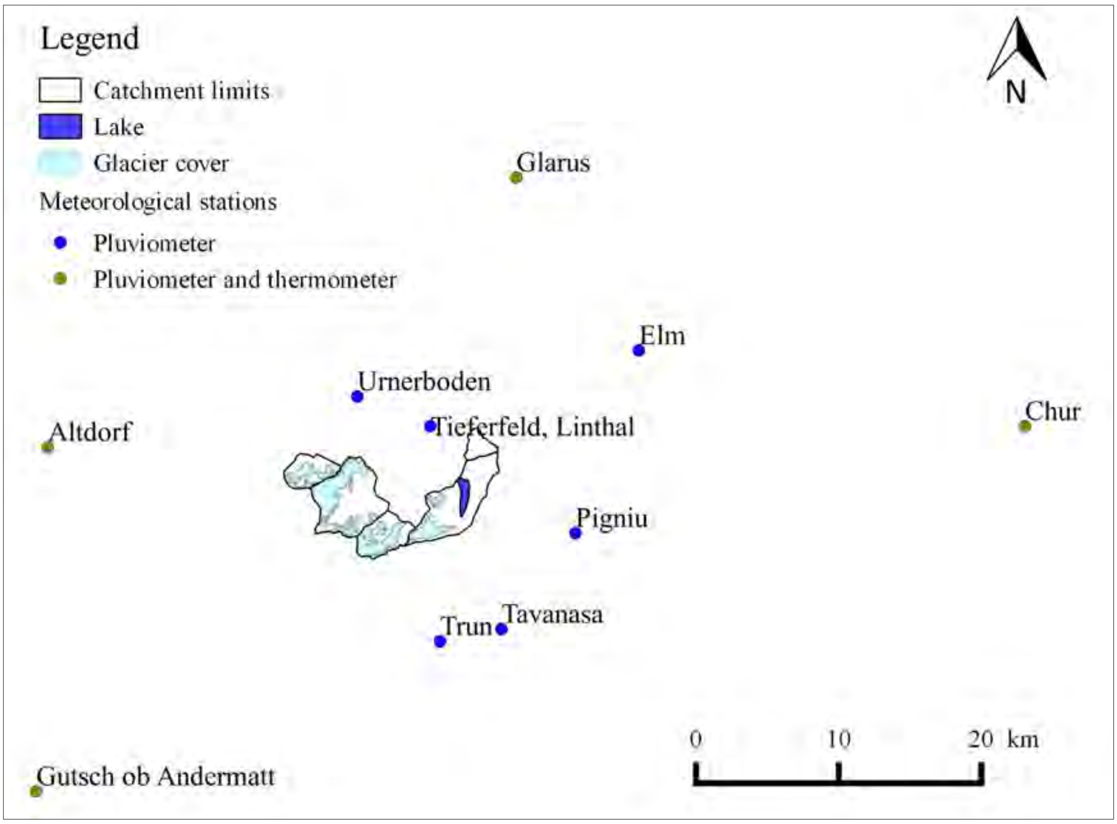

Figure 2.6: Situation of the meteorological stations in the vicinity Limmernboden catchment.

The discharge data was provided by the dam operator Kraftwerke Linth-Limmern AG (KLL) with a daily temporal resolution. The data are based on water level measurements in the reservoir and have been converted by the operator into mean daily discharge values. The covered period goes from 01/10/1997 to 31/03/2013. Figure 2.7 illustrates the discharge observation period and allows to compare it to the meteorological time series period.

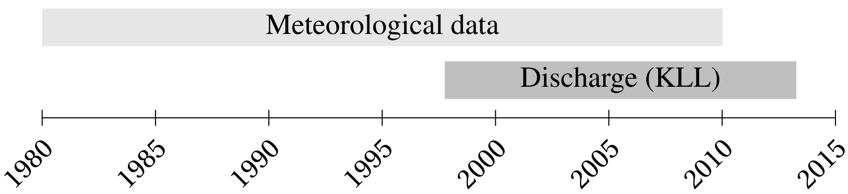

Figure 2.7: Diagram showing the periods of available meteorological and discharge data.

2.1.4 Hydrological model design

The catchment has been subdivided into altitude bands with a vertical resolution of 300 m based on a numerical terrain model with a 25 m horizontal resolution. The subdivision into altitude bands is shown in appendix in Figure A.1.

Due to the small size of the steep basin, river routing has been ignored for this model. The discharges generated by the different altitude bands are considered to sum at the outlet of the corresponding sub-basin. The inflow discharge into the Limmernboden reservoir is the sum of the different outlet discharges (from the sub-basins or the collector).

The level-volume and the level-outflow relations of the Limmernboden dam used for the simulation of the flood attenuation are shown in Figure 2.5. The initial height of the water level has been assumed to be 1857 m a.s.l. . This corresponds to full water condition and should be assumed for dam safety verifications according to SFOE (2008).

2.1.5 Model calibration and validation

The hydrological model has been calibrated and validated based on the available meteorological data as well as the discharge time series exposed in section 2.1.3. The periods considered for the calibration and the validation are respectively from 01/01/1997 to 01/10/2003 and from 01/10/2003 to 31/12/2009.

The performance coefficients (Nash-Sutcliffe efficiency, Volume ratio, Kling-Gupta efficiency) of the calibration and validation results are represented by the bar plot of Figure 2.8. The equations to estimate these coefficients are shown in appendix A.2. The optimum values of 1 is well approached by each coefficient. According to the performance coefficient qualification of Moriasi et al. (2007), the model can be qualified as very good regarding the Nash-Sutcliffe efficiency if this coefficient is larger than 0.75. In this case, the latter coefficient is larger than 0.85. The final simulation results, compared to the observations, are shown in Figure 2.9. This figure shows that the flood events are well represented, with the exception of the flood from 2001. The reason of the lack of reproduction of this flood by the model is the lack of important precipitation observations. If intense precipitation events would have been observed for the concerned period, the flood would probably have been reproduced by the model.

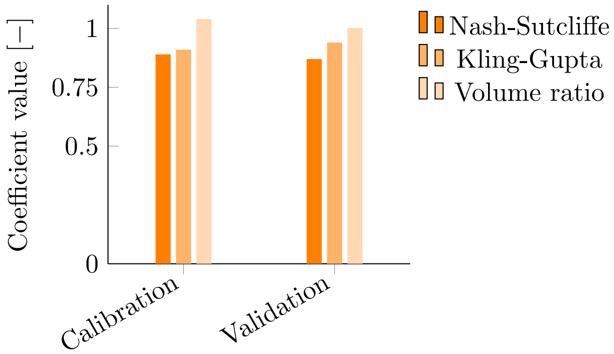

Figure 2.8: Performance coefficients proving the goodness of the hydrological model of the Limmernboden dam catchment.

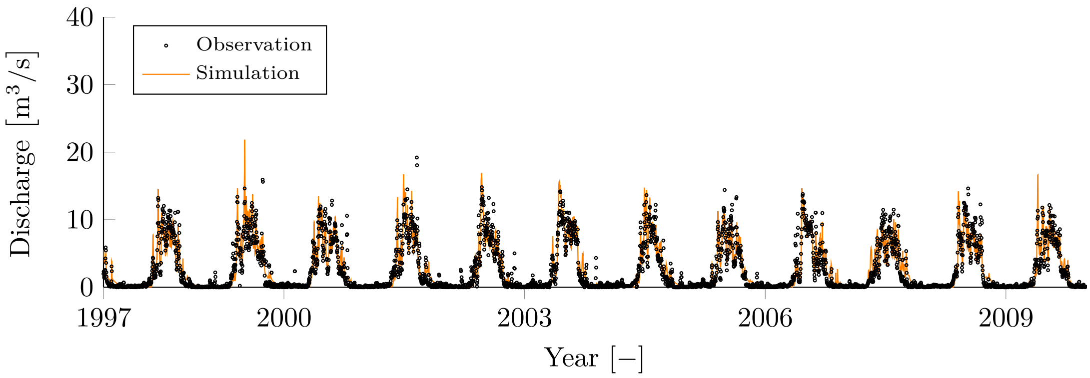

Figure 2.9: Comparison between the mean daily observed discharge and the simulation with a daily time step from 1980 to 2009 for the Limmernboden dam catchment.

2.1.6 PMP-PMF simulation

Initial conditions

The initial conditions have been deduced from a continuous simulation of the period going from 01/10/1997 to 31/12/2009. The deterministic and stochastic approach have been considered in order to compare the results.

The determined values for the deterministic approach are reported in Table 2.2. The values correspond to the 50% and 99% quantile of the simulated state variables. Under the assumption that summer conditions are necessary to generate a PMP, the estimation of the 50% and 99% quantile values has been based on the summer period (June-August). The contemplation of the initial saturation values should be made in awareness of the calibrated soil infiltration capacity $H_{GR3,max} = 0.47$ m.

For the stochastic approach, the data set has also been separated into seasonal sets. The summer time series has been retained for the determination of the initial conditions scenarios. Randomly determined moments in time have been generated and the simulated state variable values for these moments have been retained as dependent initial conditions for the simulations. A total of 5000 scenarios were generated.

Table 2.2: Summer state variable values for the 50% and 99% quantiles considered for the deterministic initialization of the hydrological model of the Limmernboden dam catchment.

Region	State variable	Symbol	50%	99%	Unit
Non glacial	Snow height	H_s	0.009	0.78	[m]
	Snow saturation	θ	0.03	0.1	[m]
	Runoff	H_r	0.004	0.021	[m]
	Soil saturation	H_{Gr3}	0.198	0.34	[m]
Glacial	Snow height	$H_{s,Gl}$	0.006	0.985	[m]
	Snow saturation	θ_{Gl}	0.01	0.1	[m]
	Glacier melt	Q_{Gl}	0.16	0.75	[m^3/s]
	Snow melt	Q_s	0.04	0.95	[m^3/s]

Temperature assumption for PMP events

The temperature attributed to the PMP events, in terms of 0°C isothermal altitude, depends on the duration of the considered event. The Limmernboden dam is situated in the northern Swiss Alps. Beside the geographical situation of the Limmernboden dam, the PMP is supposed to occur under summer conditions. The relation considered to derive the 0°C isothermal altitude for each PMP event has been derived using Equation 2.1.

$$H = ad + b \tag{2.1}$$

where H is the altitude of the 0°C isothermal altitude in [m a.s.l.], d the duration of the PMP event in [h], $a = -8.352$ [m a.s.l. / h] and $b = 4521.7$ [m a.s.l.] are the parameters determined for the northern part of Switzerland under summer conditions.

Critical wind direction

The PMP data has been elaborated by Hertig et al. (2005) for different wind directions, i.e. North, South and West-North-West. For the determination of the critical wind sector, a 3h-PMP has been randomly chosen and the corresponding PMP data was introduced in the calibrated hydrological model (initialized with the 50% quantile state variable values) in order to determine which sector generates a higher discharge than the two others.

The simulation results are shown in Figure 2.10. It can be seen that the North and the West-North-West sectors give very close estimations. The North is however slightly higher. This sector has thus been retained as the critical wind direction.

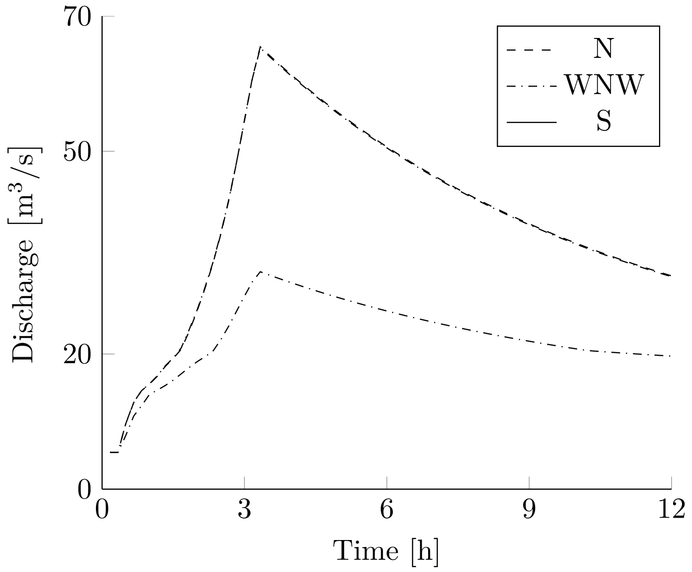

Figure 2.10: Hydrographs derived from 3h-PMPs for the three different wind sectors north (N), south (S) and west-north-west (WNW) for the Limmernboden dam catchment.

PMF estimates

In a first step, the PoMF used as upper bound for the statistical extrapolations has been estimated. The initial conditions derived from the 99% quantile values of the state variables have been used for the simulations. These values have been reported in Table 2.2. PMP events from 1h to 24h have been considered for the simulations. The maximum hourly averaged peak discharge has been derived with the moving average approach, as explained earlier. Figure 2.11 shows the maximum hourly peak discharges for the different PMP durations. The 3h PMP generated the highest hourly averaged discharge. The detailed hydrographs for the 99% quantile initial conditions are shown in Figure A.3. A comparison with the results derived from a 3h-PMP event with the stochastic approach (Figure 2.12) shows that the deterministic approach overestimates the PMF if rare initial conditions are considered, and slightly underestimates the median discharge value. This shows that the simultaneous occurrence of the 99% quantile state variable values is not accurate in this case. Due to the respect of the dependence between the state variables of the stochastic approach, the latter has been considered to estimate the upper limit for the bounded statistical extrapolation. The retained hourly averaged discharge is $Q = 275\,\mathrm{m}^3/\mathrm{s}$.

The next step is the determination of the safety flood. It has been retained in Section 1.2.6 that a flood generated under the assumption of median initial state variable values would be used for the safety verification. Figure 2.13 shows the reservoir water level estimates for different PMP durations. It can be seen that the critical PMP duration under the considered initial conditions is 23h. The corresponding inflow and outflow hydrographs as well as the reservoir level evolution are shown in Figure 2.14. It can be concluded that the safety flood generated by a 23h-PMP and median initial condition could be withstood without over-topping. The spillway capacity has not been exceeded during the simulations.

The probability of the peak discharge of the considered safety event can be derived once the statistical distribution has been fitted. For this purpose, the corresponding hourly averaged discharge has to be derived. The hourly peak discharge corresponding to the 23h-PMP event has been estimated to be $Q = 55\,\mathrm{m^3/s}$ (under median initial conditions).

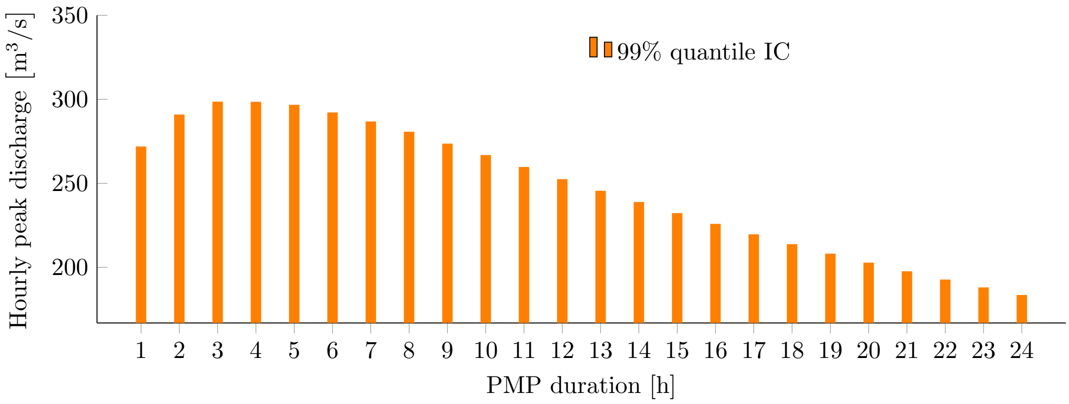

Figure 2.11: Hourly inflow peak discharges derived from different PMP events with wind sector "north" for the Limmernboden dam. "IC" stands for initial conditions.

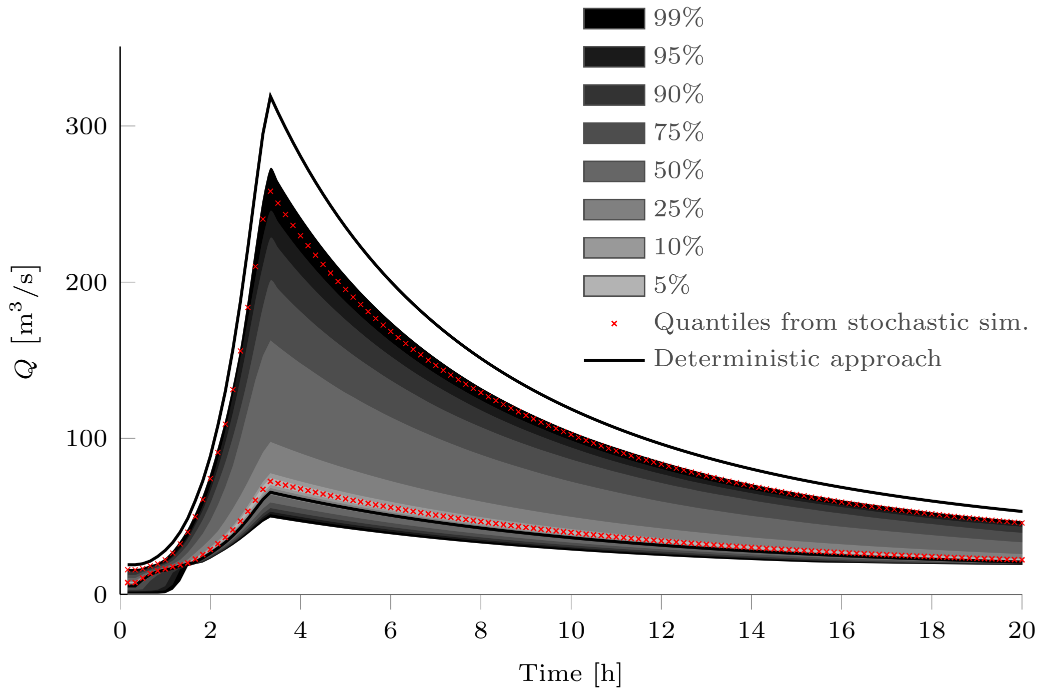

Figure 2.12: PMF estimates derived from a 3h-PMP based on 5000 initial conditions scenarios. The 50% and 99% quantile discharges are shown by the red crosses. The continuous black lines show the discharge generated when 50% and 99% quantiles for the initial state variable values were used.

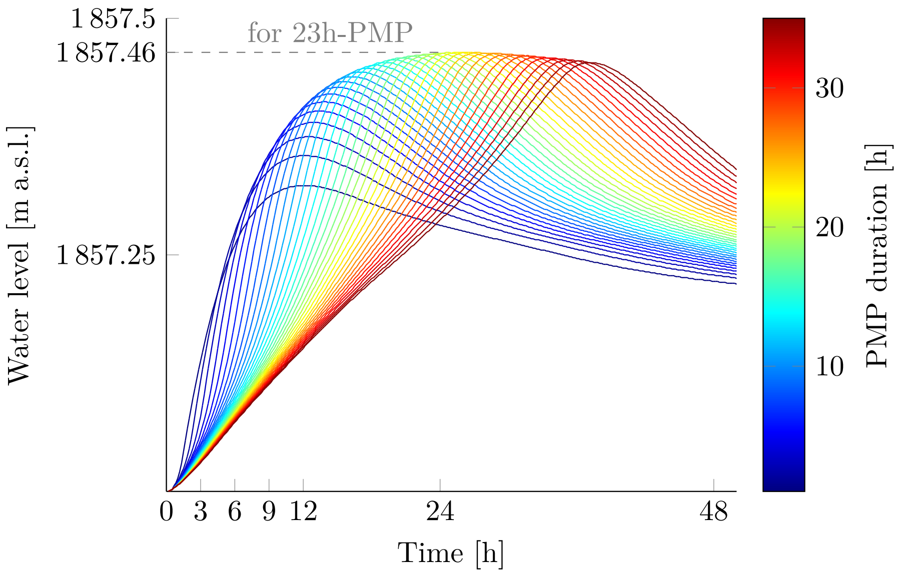

Figure 2.13: Reservoir water level estimates for the Limmernboden dam for different PMP events (wind sector "North") for 50% quantile initial values. The maximum reservoir level is reached for a 23h-PMP event.

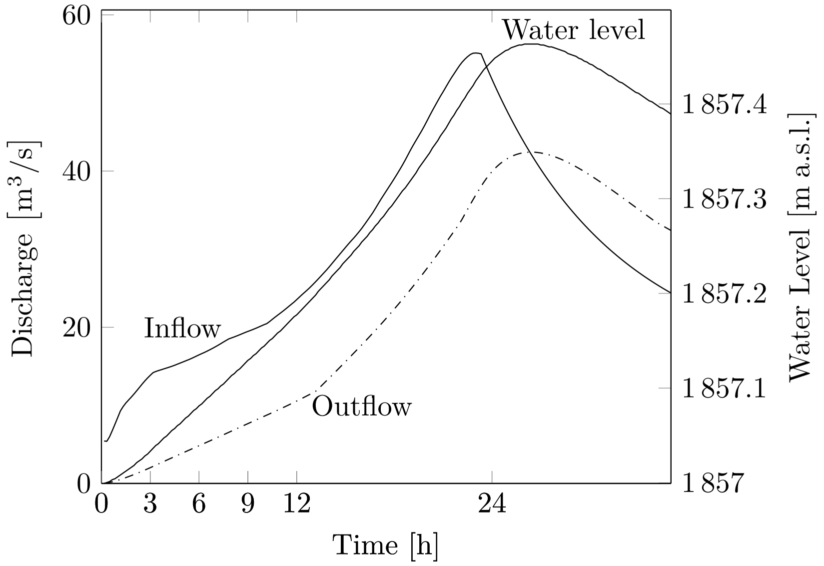

Figure 2.14: Inflow and outflow hydrographs with corresponding reservoir water level for a 23h-PMP event and median initial conditions.

2.1.7 Statistical extrapolations

The hydrological model has been used to generate the hourly maximum discharge peaks for each year. The simulation covers the period from 1980 to 2009. The resulting annual maximum values considered for the distribution fit are shown in Figure A.5. They have been fitted with a bounded distribution as well as the Log-Normal distribution and the GEV. For the POT method, a threshold of $u = 11.5\text{m}^3/\text{s}$ has been determined. This threshold was fixed in order to have at least one value per year. Furthermore, a minimum of 14 days between two peaks has been admitted to be the minimum period to guarantee independence between the events. A total of 72 peak discharges have been determined. They are highlighted in Figure A.6. This means that, on average, 2.4 values have been considered per year. According to Tavares and Da Silva (1983), the average number of events per year should be around 2, in order to get the best performance of the POT method.

The largest discharge generated by the critical PMP event has been determined to be $Q = 275\ \text{m}^3/\text{s}$. This value has been admitted as upper bound for the statistical fit. The sample skewness, estimated with Equation 2.2, is $\gamma = 0.85$. The LN4 distribution should be used in this case according to Takara and Tosa (1999). The estimated parameters for the different distribution are shown in appendix in Table A.2.

$$\gamma = \frac{1}{Ns^3} \sum_{i=1}^{N} (x_i - \bar{x})^3 \tag{2.2}$$

where x_i is an observation value, $\bar{x}$ is the mean value of the observations x_i and s is the estimate of the standard deviation of the observations.

Figure 2.15 shows the statistical extrapolations. It can be seen on this figure that the hourly peak discharge of the 23h-PMP has a return period of more than 10^{11} years according to the LN4 distribution. The other approaches (GEV, Log-normal, POT) underestimate the flood discharges compared to the LN4 distribution. The log-normal distribution is the closest to the LN4 distribution. The GEV and the POT distributions start to deviate from the LN4 distribution from a return period of 10^4 years on. This means that, up to this deviation point, the four distributions lead to very similar estimations.

According to the Swiss guidelines for dam safety (SFOE, 2008), quantity $Q_s = 1.5Q_{1000}$ can be considered as safety flood. In this case, $Q_s = 41.5$ m^3/s. The estimated discharge can be attributed a return period of approximately 10^7 according to the LN4 distribution. The safety flood derived under median initial conditions from the 23h PMP has a peak discharge that is roughly 30% higher.

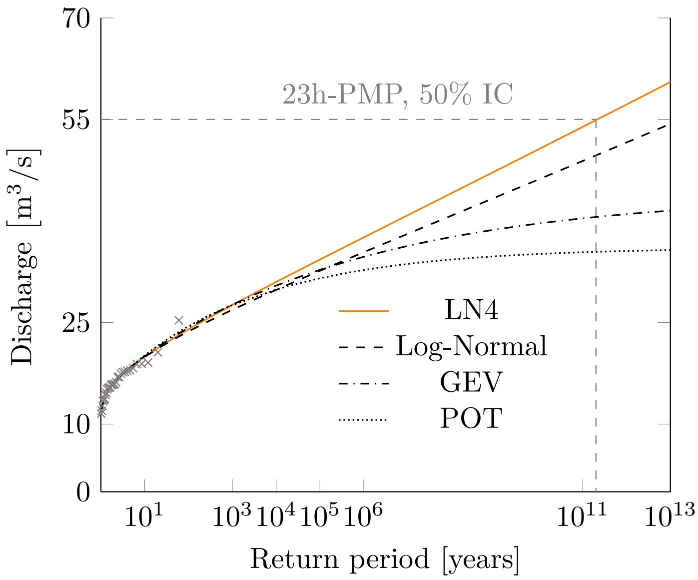

Figure 2.15: Annual maximum hourly discharge data fitted with the LN4 distribution considering an upper bound of PMF=275 m^3/s.

2.1.8 Intermediate conclusions

The case study of the Limmernboden dam could show that the upper bounded statistical distribution LN4 gave more conservative estimates than the conventional methods. Nevertheless, the spillway capacity has not been exceeded by the safety flood, that could be attributed a return period of roughly 10^{11} years. The return period of the quantity $Q_s = 1.5Q_{1000}$ has been estimated to be 10^7 years.

2.2 Application to the Mattmark dam catchment

2.2.1 Description of the Mattmark dam catchment

In this chapter, the Mattmark embankment dam (Figure 2.16) and its catchment are presented. The Mattmark dam is situated in the southern part of Switzerland in the Canton of Valais (Figure 1.1) upstream the village of *Saas Almagell* on the river *Saaser Vispa*. The limits of the catchment as well the the glacier cover and the lateral intakes are shown in Figure 2.17. The main catchment of the Mattmark reservoir, with an area of 35.6 km^2, is completed by four surrounding catchments augmenting the catchment area to 83.2 km^2. In Table 2.3, the main charatceristics of the Mattmark catchment and its reservoir are listed.

Figure 2.16: Photo of the Mattmark dam (SwissCOD, 2011).

Table 2.3: Main characteristics of the catchments and the reservoirs (SwissCOD, 2011)

Reservoirs	
Name	Mattmark
Canton	Wallis / Valais
Reservoir surface [km^2]	1.76
Volume [mio m^3]	100
Max spillway discharge [m^3/s]	230
Max discharge of ground outlet [m^3/s]	57
Spillway crest [m a.s.l.]	2197
Dam crest [m a.s.l.]	2204
Main catchment	
Area [km^2]	35.6
Glacier cover [km^2]	9.2
Primary Inflows	Stafelbach
Primary Outflows	Saaser Vispa
External catchments	
Number of additional catchments	4
Additional area [km^2]	47.6
Additional glacier cover [km^2]	20.5
Collector capacity [m^3/s]	16

2.2.2 Meteorological and discharge data

The precipitation and temperature data have been provided by MeteoSwiss. The periods covered by the meteorological time series per station are shown in Figure A.9. The detailed dates are given in Table A.3. The overlapping period of the meteorological time series is shown in Figure 2.18. The situation of the meteorological stations around the Mattmark dam are shown in Figure 2.19.

Regarding the temporal resolution of the meteorological data sets, values at a daily time step have been available at the stations measuring only precipitation (cf Figure 2.19). For the stations measuring precipitation and temperature, data at an hourly time step was accessible. The daily data has been disaggregated in hourly data sets. To do so, two nearby stations with hourly data were chosen. The data of these two stations were then interpolated using the inverse squared distance weighting, to get an estimate of hourly precipitation at the location of the station to be disaggregated. Then, the daily measured precipitation volume of the station to be disaggregated has been used to adjust the volume of the generated hourly time series.

The discharge data has been provided by the dam operator Kraftwerke Mattmark AG (KWM) with a daily time resolution. The data have been based on water level measurements in the

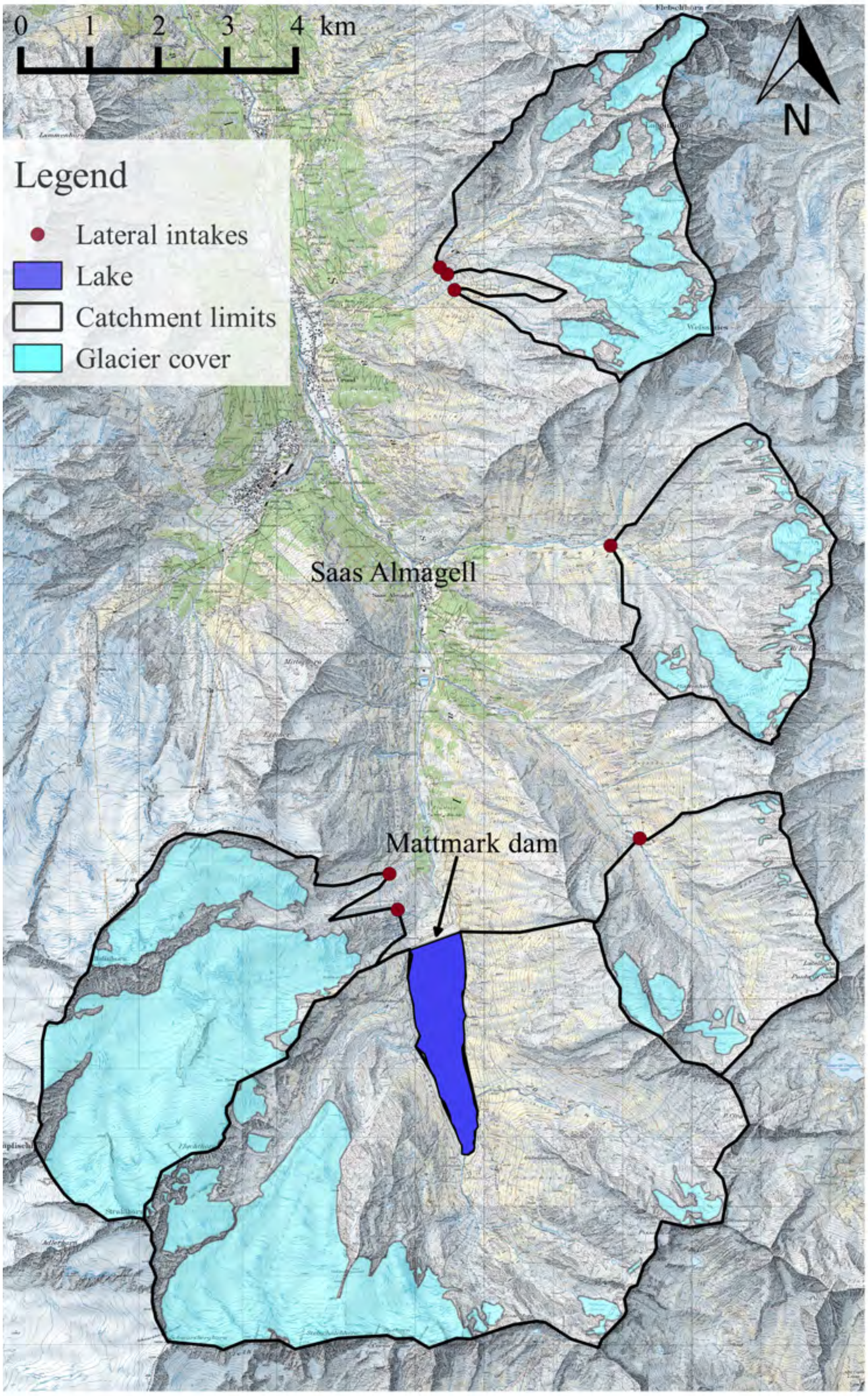

Figure 2.17: Mattmark catchment with lateral catchments, glacier covered zones and the location of the intakes.

reservoir and have been converted into mean daily discharge values. The covered period goes from 01/10/1971 to 31/05/2013. Figure 2.18 illustrates the discharge observation period and allows to compare it to the meteorological time series period.

2.2.3 Description of the spillway of the Mattmark dam

The spillway of the Mattmark dam is situated on its right bank. A sketch of the spillway is shown in Figure 2.20. The study of Boillat and Schleiss (2002) was aimed at re-evaluating and adapting the spillway capacity of the Mattmark dam. The adaptation of the original spillway is represented on the sketch of Figure 2.20. Three orifices have been introduced and the spillway crest has been elevated by 2 m. The level-outflow curve, as it has been described by Boillat and Schleiss (2002), is shown in Figure 2.21 together with the level-volume relation of the reservoir.

2.2.4 Hydrological model

The catchment has been subdivided into altitude bands with a vertical resolution of 300 m based on a numerical terrain model with a horizontal resolution of 25m . The subdivision into altitude bands is shown in Figure A.7 and A.8.

The capacity of the collector, used to derive the water coming from the lateral catchments to the Mattmark dam has been estimated to $16 m^3/s$.

Due to the small size of the basin, river routing has been ignored for this model. The discharges generated by the different altitude bands are considered to sum at the outlet of the corresponding sub-basin. The inflow discharge into the Mattmark reservoir is the sum of the different outlet discharges (from the sub-basins or the collector).

Model calibration and validation

The capability of the hydrological model to reproduce the observed discharge data is exposed in this section. As shown in Figure 2.18, the meteorological data set changed during the observation period. Therefore the performance of the model has been evaluated for the two main periods, each with invariable meteorological time series, i.e. from 1980 to 1994 (period P1) and from 1995 to 2009 (period P2). The two periods have been separated into a calibration and a validation period. For the period P1 the calibration period goes from 1987 to 1994 and the validation period goes from 1980 to 1987. For the period P2 the calibration has been made for the period from 2002 to 2009 and the model has been validated from 1995 to 2002. Figure 2.22 illustrates the performance coefficients Nash-Sutcliffe and Kling-Gupta as well as the volume ratio for the two mentioned periods P1 and P2. The equations to estimate these performance coefficients are shown in appendix A.2. The final simulation results (with the calibrated model) over the complete period and the observations are shown in Figure 2.23. It can be seen that the two major floods from

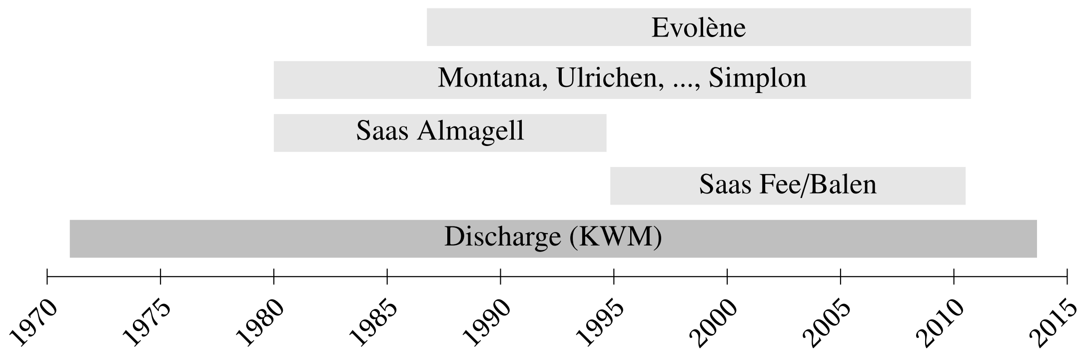

Figure 2.18: Diagram showing the periods of available meteorological discharge data.

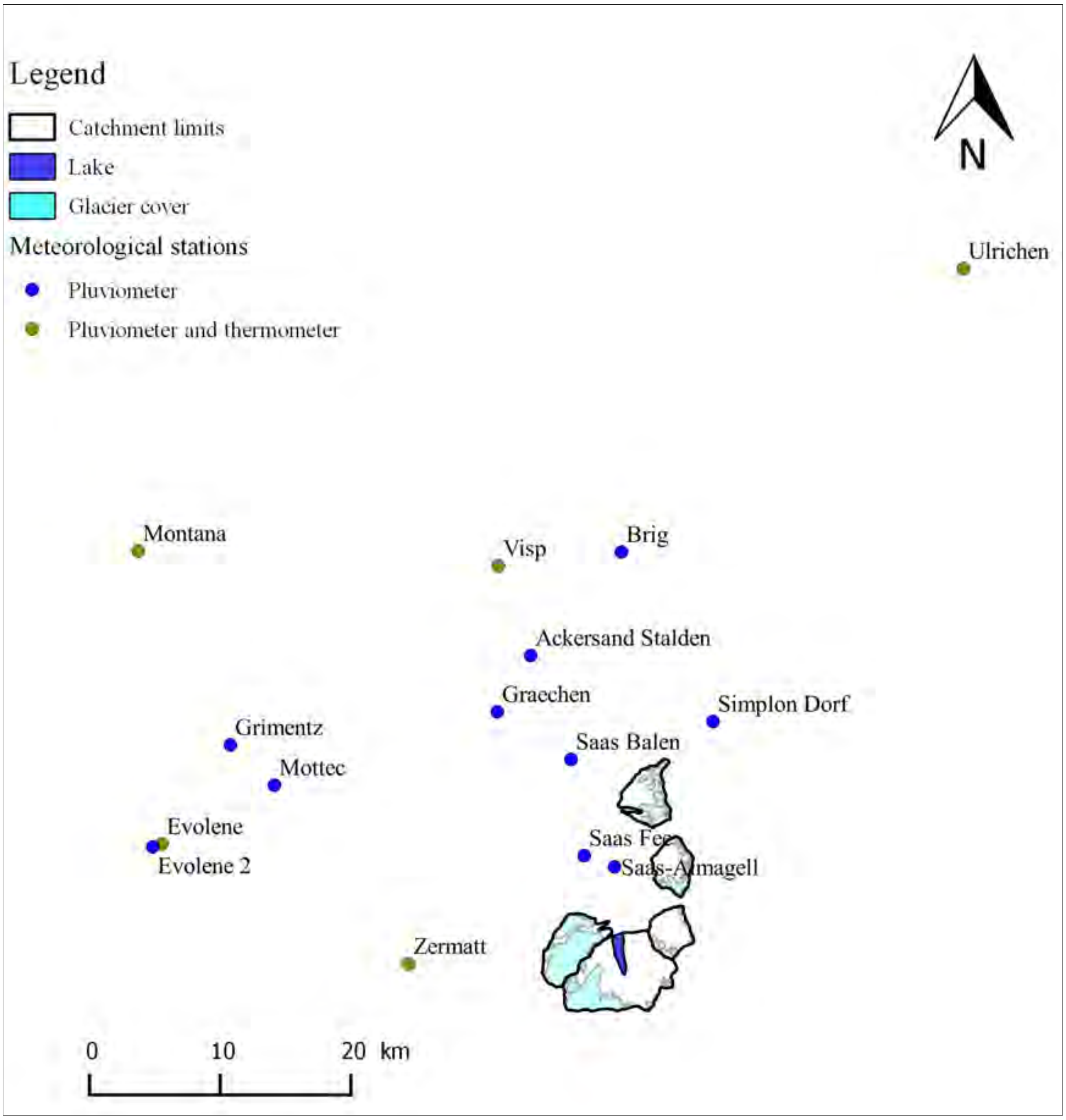

Figure 2.19: Situation of the meteorological stations in the vicinity of the Mattmark catchment.

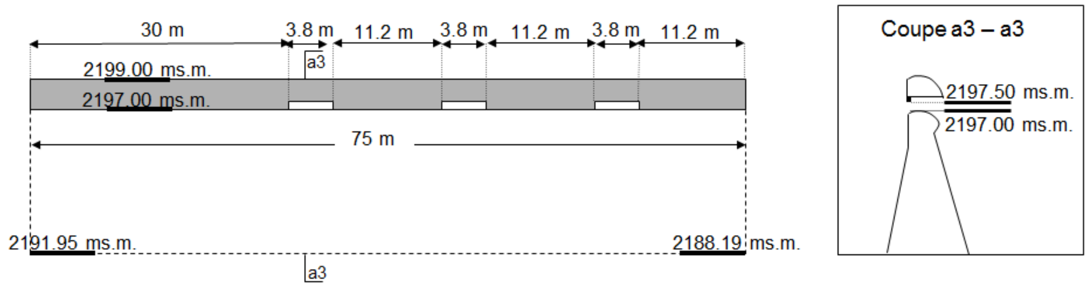

Figure 2.20: Sketch of the Mattmark spillway with lateral profile. The sketch is taken from Boillat and Schleiss (2000)

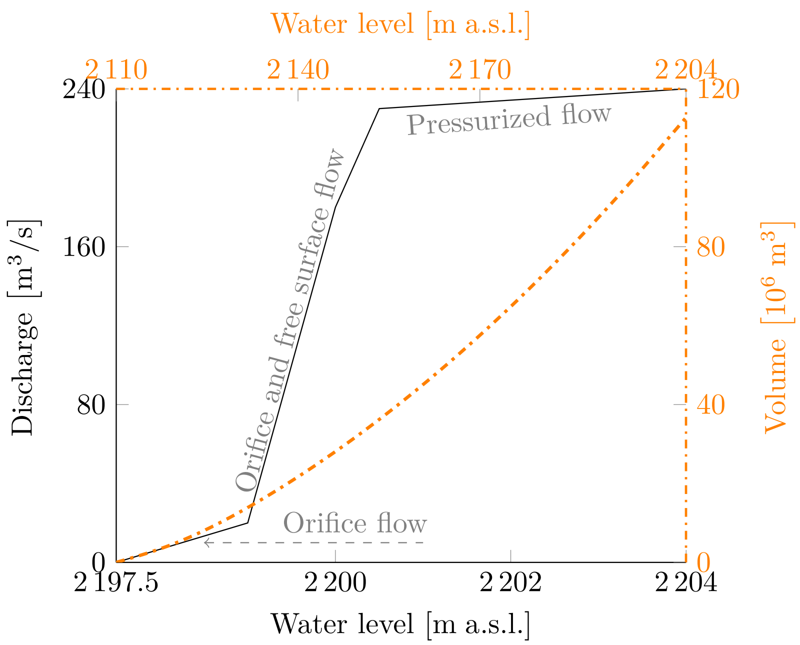

Figure 2.21: Spillway routing curve of the Mattmark dam and level-volume relation of the reservoir.

1993 and 1994 are not well represented. A comparison with the meteorological observations led to the conclusion that the measured rainfall intensities were too small to generate such high discharges. The precipitation events that caused these major flood events were probably too local to be registered by the pluviometers. However, the flood of 1993 is still represented by 70% of the observed discharge. For the flood of 1994 the model reproduced the peak discharge by 40% of the observed value.

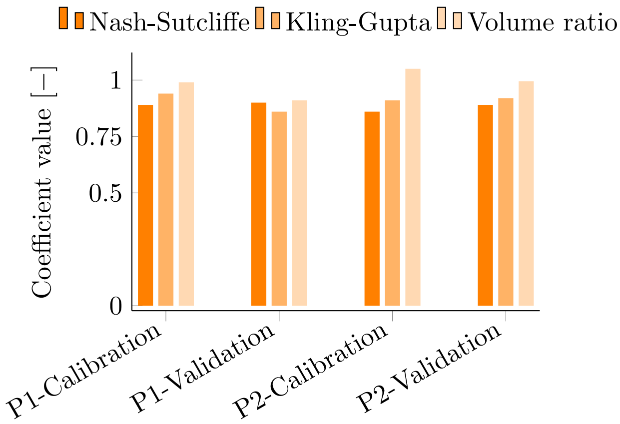

Figure 2.22: Performance coefficients proving the goodness of the hydrological model of the Mattmark dam catchment.

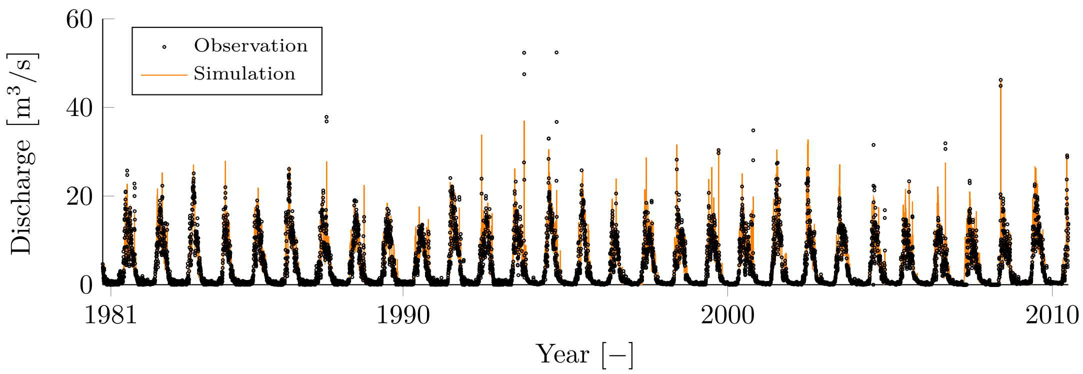

Figure 2.23: Comparison between the mean daily observed discharge and the simulation with a daily time step from 1981 to 2010.

2.2.5 PMP-PMF simulation

Initial conditions

The initial conditions for the PMP-PMF simulations have been derive by quantile analysis from the state variable values simulated during summer (June-August). The retained values are reported in Table 2.4. These values have been used to initialize the model when the deterministic approach is used. The contemplation of the initial saturation should be made being aware of the calibrated soil infiltration capacity $H_{GR3,max} = 0.28$ m.

Tthe results from the deterministic and stochastic approaches are equivalent for the Mattmark dam. Therefore only the deterministic approach is exposed in the following.

Table 2.4: Summer state variable values for the 50% and 99% quantiles considered for the hydrological model initialization.

Region	State variable	Symbol	50%	99%	Unit
Non glacial	Snow height	H_s	0.002	0.54	[m]
	Snow saturation	θ	0.009	0.097	[m]
	Runoff	H_r	0.0014	0.013	[m]
	Soil saturation	H_{Gr3}	0.081	0.18	[m]
Glacial	Snow height	$H_{s,Gl}$	0.104	0.78	[m]
	Snow saturation	θ_{Gl}	0.046	0.10	[m]
	Glacier melt	Q_{Gl}	0.299	1.19	[m^3/s]
	Snow melt	Q_s	0.182	2.02	[m^3/s]

Temperature for PMP events

The temperature attributed to the PMP events, in terms of 0°C isothermal altitude, has been derived using Equation 2.3.

$$H = ad + b \tag{2.3}$$

where H is the altitude of the 0°C isothermal altitude in [m a.s.l.], d the duration of the PMP event in [h], $a = -11.554$ [m a.s.l. / h] and $b = 4815.2$ [m a.s.l.] are the parameters for the southern part of Switzerland under summer conditions.

Critical wind direction

The most critical wind sector of the PMP maps had to be determined. For this purpose, a 3h-PMP event has been extracted from the PMP maps for the three available wind directions. The three events have been used to derive the PMF with the calibrated hydrological model. The PMP data have been temporally distributed using the 5% quantile rainfall mass curve exposed in the methodology description. The simulations were performed with a time step of 10 minutes. The PMP event that led to the highest PMF discharge has been considered to determine the most critical wind direction and thus the PMP maps that have been retained for the following simulations. The hydrographs derived from the three 3h-PMP events are represented in Figure

2.24. It can be seen that the most critical wind sector is "south".

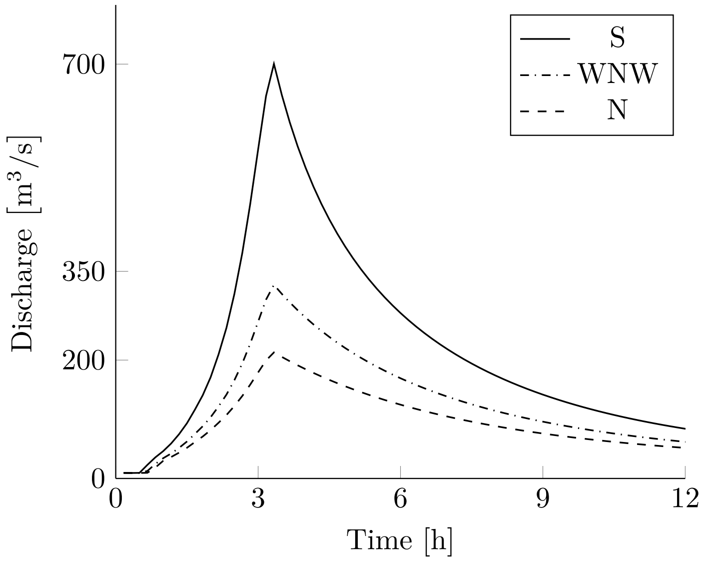

Figure 2.24: Hydrographs derived from 3h-PMPs for three different wind sectors: north (N), south (S) and west-north-west (WNW).

PMF estimates

The PMP maps used for the following simulations are the maps generated for the wind sector "south". The deterministic approach has been used to determine the critical PMP duration. The PMP-PMF simulations were performed with a 10 minutes time step.

First, the PoMF, used as upper bound for the statistical extrapolations, has been determined. The initial conditions have been derived from the 99% quantile values of the state variables. They are reported in Table 2.4. The hourly maximum peak discharges have than been derived calculating the hourly average with gliding window of a one hour width. Figure 2.25 shows the maximum hourly peak discharges for the different PMP durations. The detailed hydrographs for the different PMP durations are shown in Figure A.10. The 3h-PMP generated the highest hourly peak discharge when considering the 99% quantile for the initial value determination. The value of $Q = 1000\,\mathrm{m^3/s}$ has been retained as upper bound for the statistical fit, performed below in section 2.2.6.

The next step is to determine the safety flood. It has been retained that the median state variable values would be admitted for the estimation of the safety flood. The PMP duration leading to the highest peak discharge is not necessarily the most critical for the dam and the spillway when the initial conditions change. The simulations of the reservoir level showed that the critical PMP for the dam has a duration of 16h (time step: 10 minutes, 50% quantile initial conditions). Figure 2.26 shows the simulation results. The corresponding inflow and outflow hydrographs as well as the water level evolution are shown in Figure 2.27. The hourly averaged discharge peak value has been estimated to be $Q = 450\,\text{m}^3/\text{s}$.

From the shape of the outflow hydrograph and the level-outflow curve (Figure 2.21), it can be deduced that the spillway conduit was pressurized at a certain moment. For the 50% quantile initial values, the critical event was a 16h-PMP. From Figure 2.27, it could be deduced that the outflow conduit was also pressurized for this event.

Finally, it can be retained that the safety flood generated by a 16h-PMP and median initial condition would not lead to overtopping. It would not even occur for the 99% quantile initial values, for which a PMP duration of 13h is critical for the reservoir water level. The water level evolution estimates for different PMP durations are shown in Figure 2.26. The inflow and outflow hydrographs of the scenario with 99% quantile initial conditions are shown in Figure A.13. The hourly averaged peak discharge (for a 13h-PMP and the 99% quantile initial conditions) has been estimated to be $Q = 620\,\text{m}^3/\text{s}$.

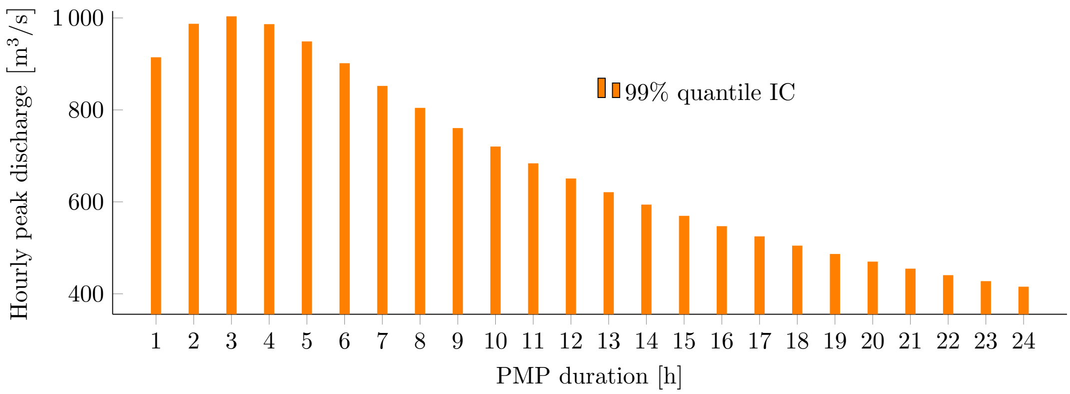

Figure 2.25: Hourly inflow peak discharges derived from different PMP events with wind sector "south". "IC" stands for initial conditions.

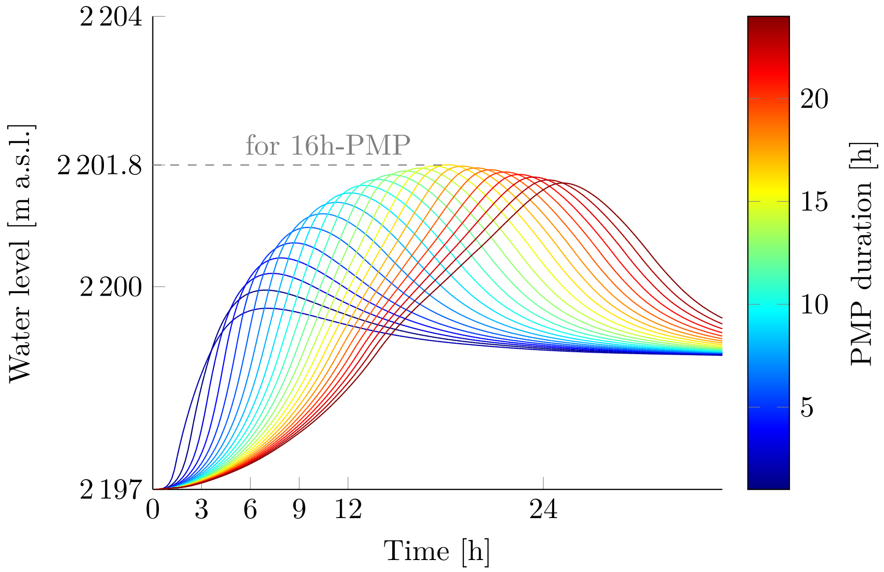

Figure 2.26: Reservoir water level for different PMP events (wind sector "south") for 50% quantile initial values. The maximum level is reached for a 16h-PMP event.

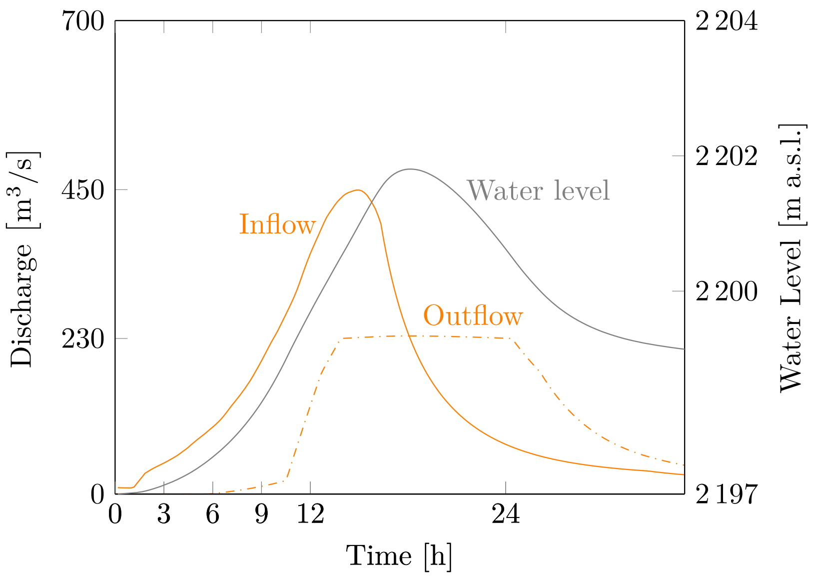

Figure 2.27: Reservoir water level for different PMP events (wind sector "south") for 50% quantile initial values. The maximum level is reached for a 16h-PMP event.

2.2.6 Statistical extrapolation acounting for the estimated PMF

The hydrological model has been used to generate the annual maximum values with an hourly temporal resolution. Figure 2.23 showed, however, that the two major floods from 1993 and 1994 have not been well represented by the model. The flood estimations underestimate these observations. Boillat and Schleiss (2002) presented reconstructed hydrographs of the two mentioned floods with an hourly time step. The reconstruction was based on data sets of the turbined water volumes and the reservoir level measurements. The peak discharges of these two reconstructed floods have been used to replace the simulated values under the assumption that the detailed analysis of the two mentioned floods, performed by Boillat and Schleiss (2002), better represents the real hourly discharge. The generated data set, used for the fit of the statistical distributions, is shown in Figure A.14. These data have been fitted with the log-normal distribution as well as the GEV and a bounded distribution. For the POT method, a threshold of $u = 26\mathrm{m}^3/\mathrm{s}$ has been determined. This threshold was fixed in order to have at least one value per year. Furthermore, a minimum of 10 days between two peaks has been admitted to be the minimum period to guarantee independence between the events. A total of 87 peak discharges have been determined like this. They are highlighted in Figure A.15. This means that, on average, 2.8 values have been considered per year. According to Tavares and Da Silva (1983), the average number of events per year should be around 2, in order to get the best performance of the POT method. Madsen (1996) concluded that good performances of the POT method can be awaited when the threshold definition results in 2 to 5 values per year.

In Section 2.2.5, the PMF has been estimated to be 1000 m^3/s. This quantity is considered as upper limit for the statistical extrapolation. The sample skewness of the yearly maximum discharge values has been estimated with Equation 2.2. The results, $\gamma = 2.75$, led to the conclusion that, according to Takara and Tosa (1999), the EV4 distribution is most appropriate for the extrapolations. The fitted EV4 distribution is shown in Figure 2.28. The estimated parameters for the different distribution are shown in appendix in Table A.4.

The two above exposed scenarios, i.e. 50% and 99% initial values, with critical PMP durations of 16h and 13h led to maximum hourly average discharge of 450 m^3/s and 620 m^3/s. The statistical extrapolation shown in Figure 2.28 could be used to attribute return periods to the hourly averaged maximum discharges. The 16h-PMP combined with initial conditions being the median values of the state variable values, led to a discharge of 450 m^3/s. The attributed return period is $0.7 \cdot 10^5$ years, according to the EV4 distribution. For the scenario with 99% quantile initial conditions, the derived discharge for a 13h-PMP was 620 m^3/s. The return period of this discharge was estimated to be $0.7 \cdot 10^6$ years, according to the EV4 distribution.

The extrapolation using conventional statistical approaches show significant differences compared to the EV4 distribution. The log-normal distribution is clearly not adapted to fit the data. The extrapolations using GEV and POT show similar shapes. The latter reach the upper bound for return periods of roughly 10^5 to 10^8 years. Due to the slope of the extrapolation curves, a small increase of the return period would induce to highly increase the discharge estimation. Estimation way above the estimated upper bound would thus be possible even for return periods smaller than 10^6 years (considering the GEV distribution), what is clearly a contradiction to the PMP-PMF approach. The GEV and POT can therefore be assumed to unrealistically approach the deterministically determined upper bound. Furthermore, the GEV is returning considerably higher discharge values than the POT method for the same return periods. The EV4 is situated in between the GEV and POT estimations. Around return periods of 10^7, the EV4 starts to flatten in order to approach the upper bound.

According to the Swiss guidelines for dam safety (SFOE, 2008), quantity $Q_s = 1.5Q_{1000}$ can be considered as safety flood. In this case, $Q_s = 283.5\ \mathrm{m^3/s}$. The estimated discharge can be attributed a return period of slightly than 10^4 years according to the EV4 distribution. The safety flood derived under median initial conditions from the 16h PMP has a peak discharge that is roughly 60% higher.

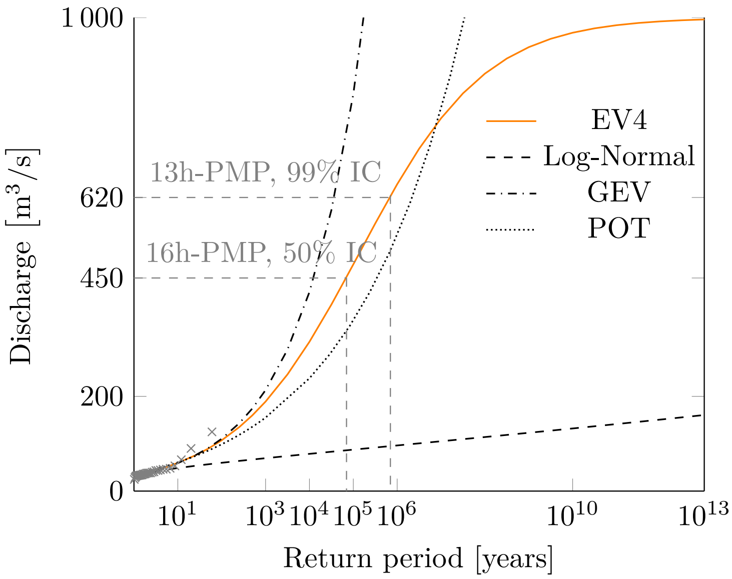

Figure 2.28: Annual maximum hourly discharge data fitted with the EV4 distribution considering an upper bound of PMF=1000 $\mathrm{m^3/s}$.

2.2.7 Intermediate conclusions

It can be concluded that the CRUEX++ methodology led to plausible flood estimates compared to the GEV and POT. As such, it could be successfully applied to the medium size catchment of the Mattmark dam. The simulations allowed to derive the critical combination between assumed initial conditions and the PMP duration after the critical wind sector had been determined. The maximum generated discharge value under very severe initial conditions (99% quantile) has been retained as upper bound for the application of the upper bounded statistical distribution. The extrapolation with the EV4 distribution allowed to attribute return periods to the to simulated scenarios. The return periods of the critical event discharges could be estimated to vary from roughly 10^5 to 10^6 when the initial conditions vary 50% quantile to 99% quantile.

2.3 Application to the Contra dam catchment

The Contra dam catchment has an area of 233 km^2, which it is theoretically outside of the application bounds of the CRUEX++ methodology (230 km^2). The application is nevertheless performed. Therefore, the results have to be contemplated under reserve and do not allow to definitely conclude on an insufficient spillway capacity if the latter would result from the calculations. It can be expected that the precipitation is overestimated since the spatial PMP coverage is slightly to high. The analysis illustrates what could be the observations when the methodology is applied on a catchment with a surface being at the application limits of the CRUEX++ methodology.

2.3.1 Description of the catchment of the Contra dam

In this section, the Contra concrete dam (Figure 2.29) and its catchment are presented. The Contra dam is located in the Souther Alps in the canton of Ticino (Figure 1.1). A detailed representation of the main catchment, with an area of 233 km^2, and the discharge measurement stations is presented in Figure 2.30.

Figure 2.29: Photo of the Contra dam (SwissCOD, 2011).

The Contra dam is not connected to lateral intakes and no glacier cover is present or has been present since the beginning of the discharge measurements in the basin. The altitude range of the catchment reaches from around 470 m a.s.l. at reservoir level up to 2864 m a.s.l., the summit called Pizzo Barone. The spillway capacity of the Contra arc dam is 2150 m^3/s according to SwissCOD (2011). The main characteristics of the Contra dam and its catchment are summarized in Table 2.29.

Table 2.5: Main characteristics of the Contra dam catchment and the reservoir (SwissCOD, 2011)

Reservoirs	
Name	Contra
Canton	Tessin / Ticino
Reservoir surface [km^2]	1.68
Volume (without the volume reserved for sediments) [mio m^3]	94.1
Max spillway discharge [m^3/s]	2150
Max discharge of ground outlet [m^3/s]	340
Spillway crest [m a.s.l.]	470
Dam crest [m a.s.l.]	473.5
Main catchment	
Area [km^2]	233
Glacier cover [km^2]	0
Primary Inflows	Verzasca
Primary Outflows	Verzasca

2.3.2 Meteorological and discharge data

The meteorological data has been provided by MeteoSwiss. For the present study, 11 meteorological stations have been taken into account. At all stations precipitation has been measured, but only at 5 stations temperature measurements have been performed. The overlapping measurement period of the different stations goes from 01/01/1981 to 30/11/2014. Figure A.17 illustrates the periods covered by the meteorological time series for each station. The detailed dates of the begin and end of the time series are given in Table A.5.

Regarding the temporal resolution of the meteorological data sets, values at a daily time step have been available at the stations measuring only precipitation (cf Figure 2.32). For the stations measuring precipitation and temperature, data at an hourly time step was accessible. The daily data has been disaggregated in hourly data sets. To do so, two nearby stations, for which hourly data have been available, had to be chosen. The data of these two stations were then interpolated, using the inverse squared distance weighting, to get an estimate of hourly precipitation at the location of the station to be disaggregated. Finally, the daily measured precipitation volume of the station to be disaggregated has been used to adjust the volume of the generated hourly time series.

The discharge data have been provided by the dam operator Verzasca SA with a daily time step. The covered period reaches from 01/01/1968 to 31/12/2014. Furthermore, hourly measurements have been obtained at two discharge measurement stations handled by the Federal Office for the

Environment (FOEN). These two stations, named Campioi-Lavertezzo and Riale di Pinascia, are situated on the map of Figure 2.30. The periods that have been available from these stations go from 01/09/1989 to 01/11/2014 for Campioi-Lavertezzo and from 01/07/1992 to 01/11/2014 for Riale di Pinascia. Figure 2.31 illustrates the discharge observation periods and allows to compare it to the overlapping period of the considered meteorological stations.

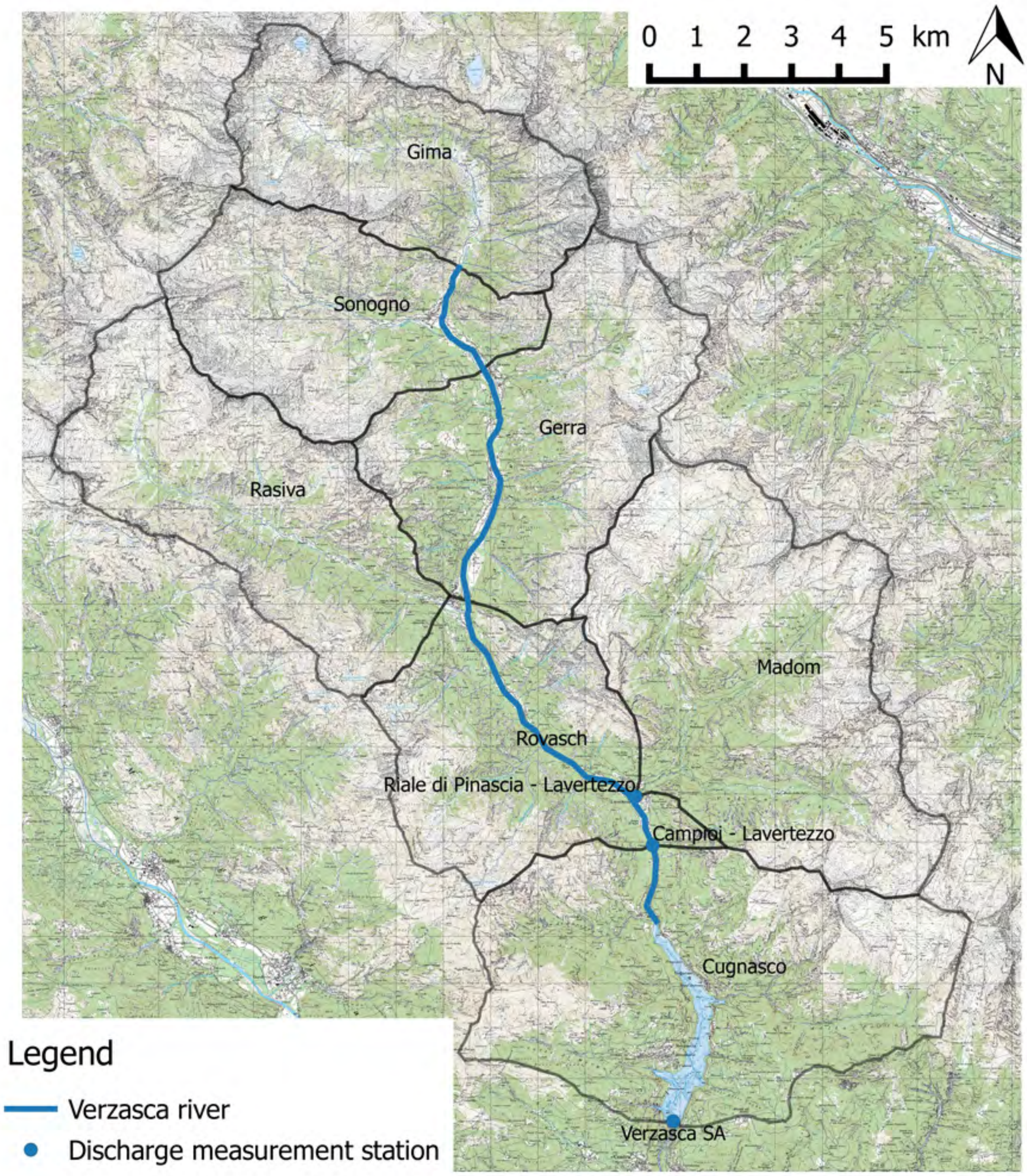

Figure 2.30: Contra dam catchment with discharge measurement stations.

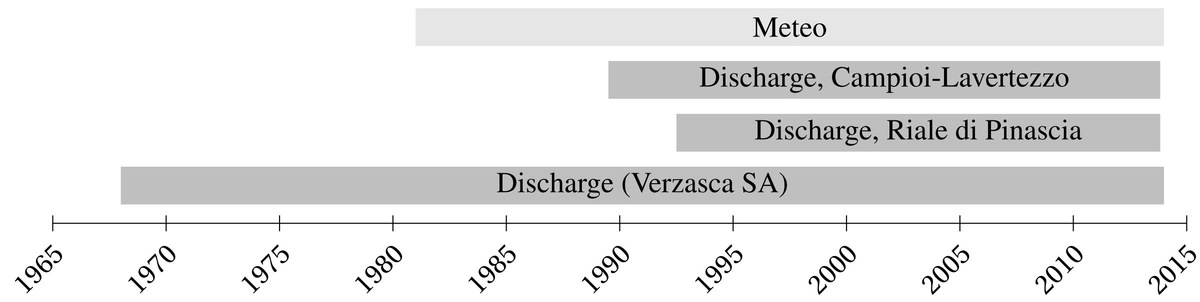

Figure 2.31: Diagram showing the periods of available meteorological and discharge data for the Contra dam modelisation.

2.3.3 Description of the spillway

The spillway of the Contra dam is integrated in the concrete structure. It is composed of 12 standard spillways, 6 on the right and 6 on the left side of the dam. The spillway has been adapted in 1994. The works have been described by Bremen and Bertola (1994). Figure 2.33, taken from the ICOLD publication of Bremen and Bertola (1994), shows that the spillway crest is at 470 m a.s.l. . Three meters higher, the road passing above the spillway limits the free surface flow of the spillway to a water level of 474.5 m a.s.l ($= 470 + \frac{3}{2}h_{cr}$; $h_{cr} = 3$ m being the admissible critical height). Pressurized orifice flow has been admitted for water levels between 474.5 to 474.93 m a.s.l. Above 474.93 m a.s.l., overtopping occurs parallel to pressurized orifice flow. The level outflow relation is plotted together with the level-volume relation in Figure 2.34.

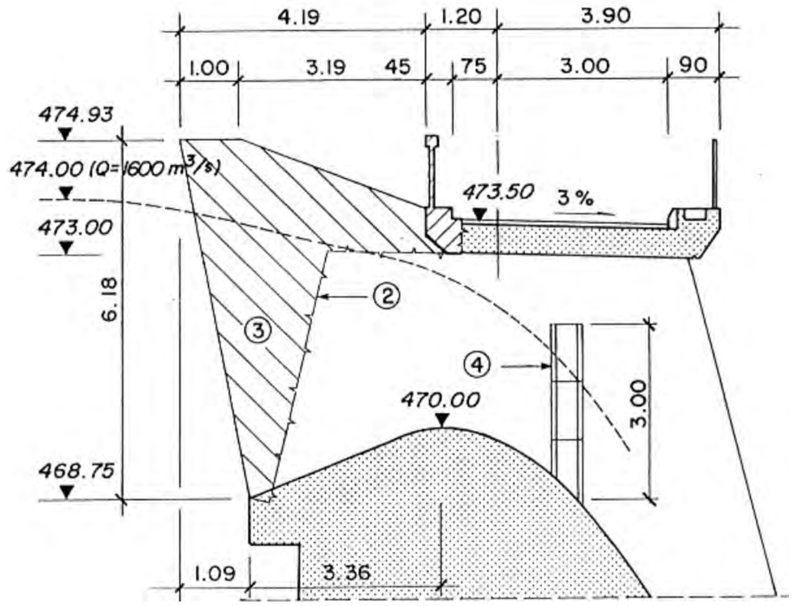

Figure 2.33: Profile of the spillway crest of the Contra dam. The illustration has been published by Bremen and Bertola (1994).

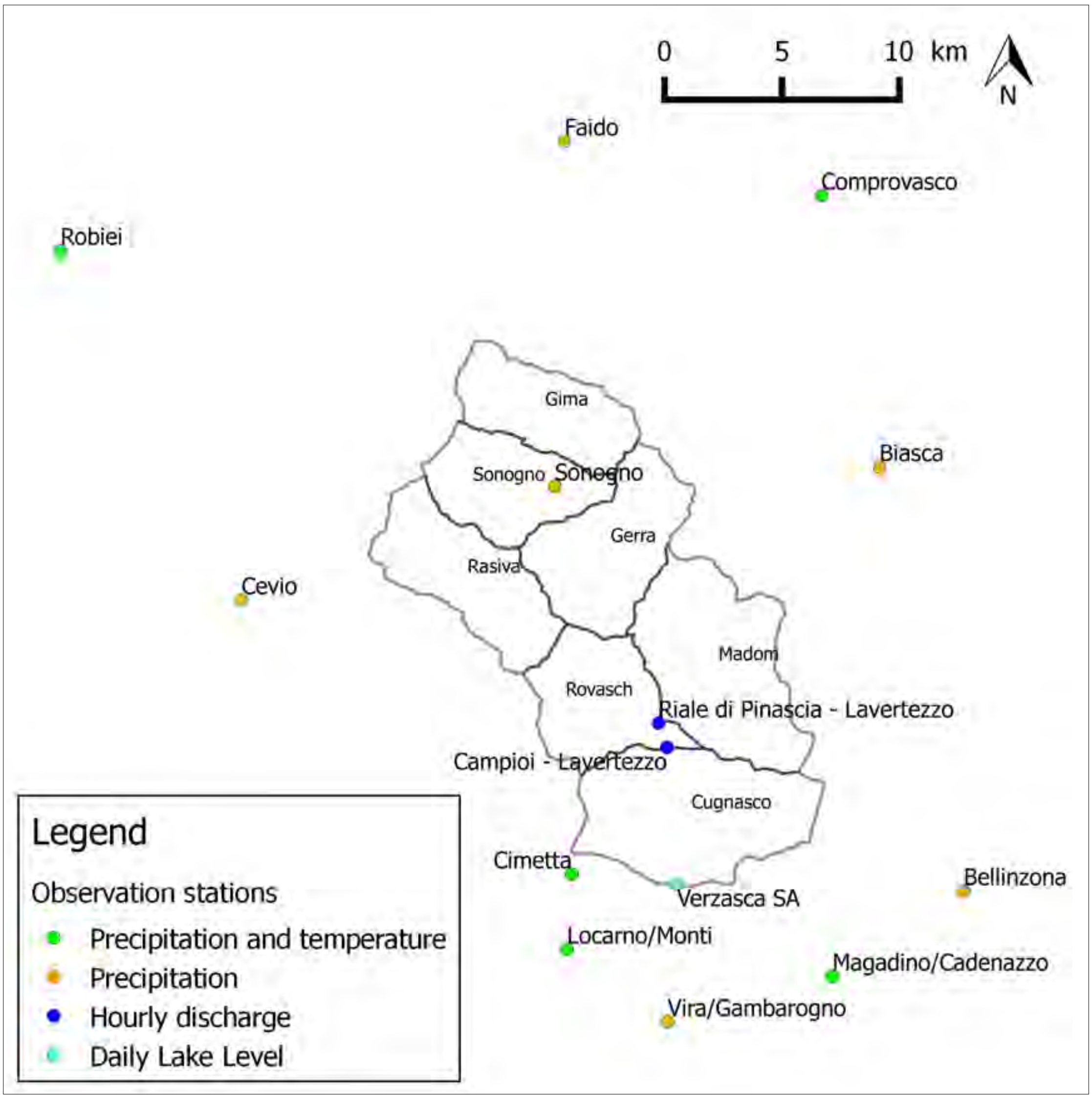

Figure 2.32: Contra dam catchment with discharge and meteorological observation stations.

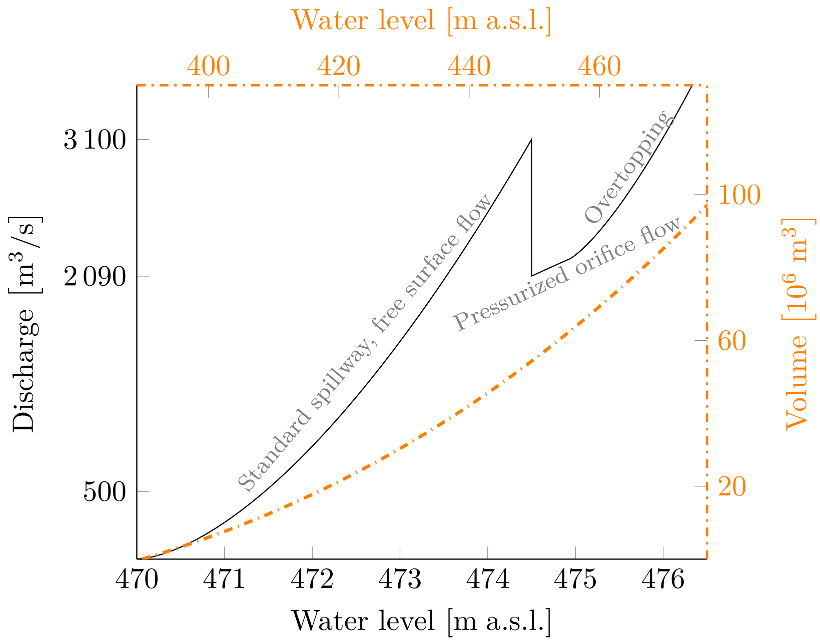

Figure 2.34: Spillway routing curve of the Contra dam and level-volume relation of the reservoir.

2.3.4 Hydrological model design

Due to the considerable size of the catchment, sub-basins have been determined based on topographic maps. Then each sub-basin has been subdivided into altitude bands with a vertical resolution of 300m based on numerical terrain model with a horizontal resolution of 25m. The subdivision in sub-basins is shown in Figure 2.30, the altitude bands are illustrated in Figure A.16. The discharges generated by the different altitude bands are considered to sum at the outlet of the corresponding sub-basin. The outflow of each sub-basin is routed towards the reservoir using the kinematic wave approach.

The level-volume and the level-outflow relation of the Contra dam used for the simulation of the flood attenuation are shown in Figure 2.34. The initial height of the water level has been assumed to be 470 m a.s.l. . This corresponds to full water condition and should be assumed for dam safety verifications according to SFOE (2008).

2.3.5 Model calibration and validation

The hydrological model has been calibrated and validated based on the available meteorological data as well as the discharge time series presented earlier. Due to the availability of discharge measurements at three different locations, it was possible to subdivide the catchment into three zones. Each zone has been calibrated and validated based on the discharge observations from the closest downstream measurement station.

The calibration period for the three zones goes from 01/10/2003 to 30/09/2014. The validation periods depend on the measurement station. For Campioi-Lavertezzo, the validation period goes from 09/01/1989 to 01/10/2003. The calibrated zone has a surface of 142km^2. For the Riale di Pinascia, the calibration has been validated for the period going from 01/07/1992 to 01/10/2003. The concerned zone has a surface of 44km^2. The validation of the calibration of the zone downstream of the two above mentioned stations has been performed on the daily data set provided by Verzasca SA and covers the period going from 01/01/1981 to 01/10/2003. The surface of the calibrated zone is 47km^2.

The performance coefficients (Nash-Sutcliffe efficiency, Volume ratio, Kling-Gupta efficiency) of the calibration and validation results represented in Figure 2.35 prove that the optimum values of 1 is well approached by each coefficient for each of the three zones. According to the performance coefficient qualification of Moriasi et al. (2007), the model can be qualified as very good regarding the Nash-Sutcliffe efficiency if this coefficient is larger than 0.75. For the observation station Riale di Pinascia, the Nash-Sutcliffe efficiency is less good than for the two other zones. However, this zone has still a good Kling-Gupta efficiency and the volume ratio is as good as for the other two zones. All in all, the performance coefficients let conclude that the model has been well calibrated. The final simulation results compared to the observations are shown in Figure 2.36. It can be seen that the flood events are well represented, with the exception of the flood from 2001. The reason of the lack of reproduction of this flood by the model is the lack of important precipitation observations. If intense precipitation events would have been observed for the concerned period, the flood would probably have been reproduced by the model.

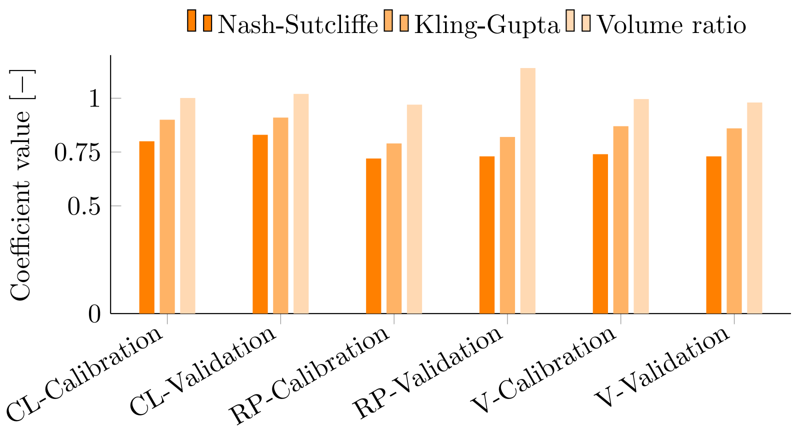

Figure 2.35: Performance coefficients proving the goodness of the hydrological model of the Contra dam catchment. "CL" stands for the station Campioi-Lavertezzo, "RP" for the station Riale di Pinascia and "V" stands for Verzasca SA (inflow discharge deduced from reservoir level measurements).

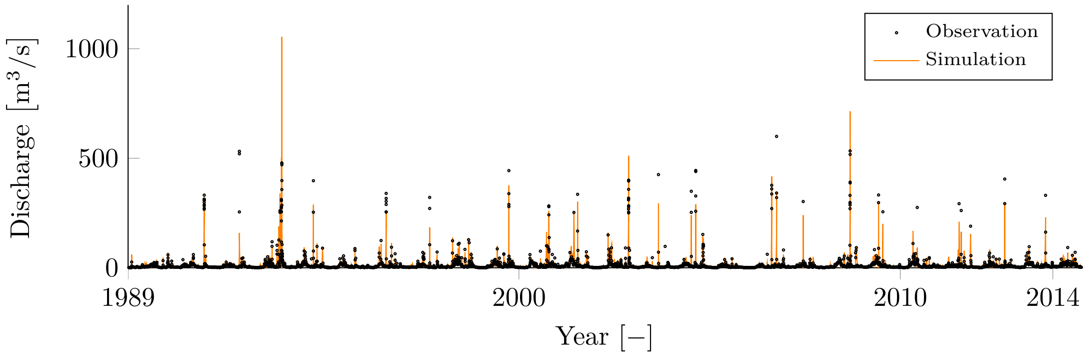

(a) Observations and simulation results with an hourly time step at the discharge measurement station Campioi -Lavertezzo.

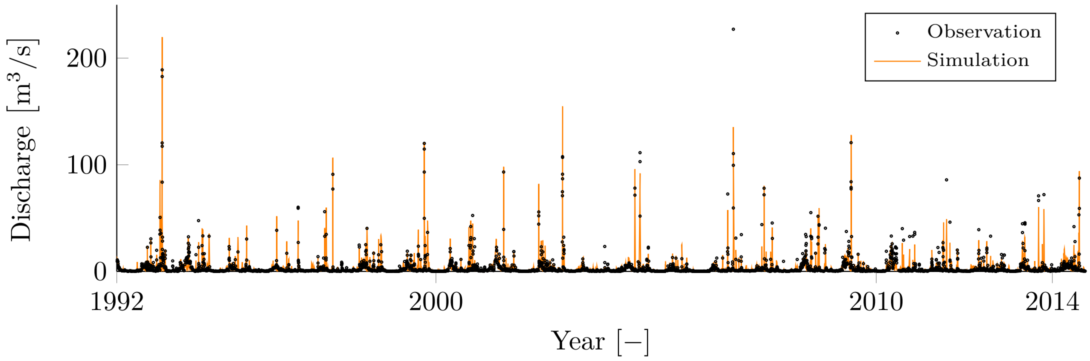

(b) Observations and simulation results with an hourly time step at the discharge measurement station Riale di Pinascia.

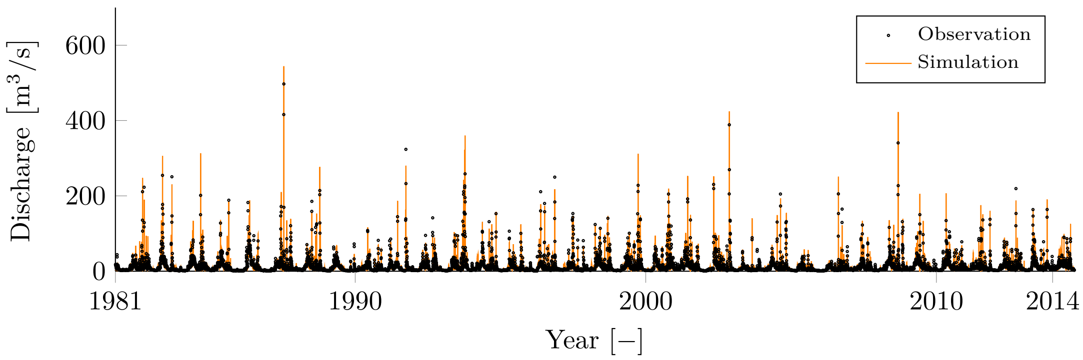

(c) Observations and simulation results with daily time step at the for the inflow discharge into the Contra dam reservoir (Verzasca SA measurements).

Figure 2.36: Comparison between observed discharges and the simulation for the three discharge observation stations, i.e. Campioi-Lavertezzo, Riale di Pinascia and Verzasca SA data.

2.3.6 PMP-PMF simulation

Initial conditions

The initial conditions for the PMP-PMF simulations have been derived by quantile analysis from the state variable values simulated during summer (June - August). The retained values are reported in Table 2.6. It has been distinguished between the different sub-basins due to the important size of the basin. The contemplation of the initial saturation should be made being aware of the calibrated soil infiltration capacity $H_{GR3,max} = 0.4$ m for the sub-basin Madom, $H_{GR3,max} = 0.26$ m for the sub-basin called Cugnasco and $H_{GR3,max} = 0.26$ m for the remaining sub-basins. The values in Table 2.6 indicate very small to non-existent initial snow cover. Therefore, the soil saturation can be considered as main driver among the initial state variables. Consequently, the stochastic approach has not been considered; it can be assumed to return very similar results compared to the deterministic approach.

Temperature for PMP events

The 0°C isothermal altitudes attributed to the PMP events have been derived using Equation 2.4.

$$H = ad + b \tag{2.4}$$

where H is the altitude of the 0°C isothermal altitude in [m a.s.l.], d the duration of the PMP event in [h], $a = -11.554$ [m a.s.l. / h] and $b = 4815.2$ [m a.s.l.] are the parameters for the southern part of Switzerland under summer conditions.

Critical wind direction

The PMP maps have been derived for three different wind sectors. One of these sectors should lead to the most severe PMP event. Figure 2.37 shows the hydrographs derived from a 3h PMP, median initial conditions and temperature conditions corresponding to an isothermal altitude of 4780 m a.s.l.. It can be seen, that in the case of the Contra dam catchment, the highest discharge and volume has been generated by the maps corresponding to the sector "south". The sectors "west-north-west" and "north" return nearly the same results that are considerable lower than the estimates based on the sector "south".

Table 2.6: Summer state variable values (equivalent water height) for the 50% and 99% quantiles considered for the deterministic initialization of the hydrological model of the Contra dam catchment.

Region	State variable	Symbol	50%	99%	Unit
Madom	Snow height	H_s	0	0	[m]
	Snow saturation	θ	0	0	[m]
	Runoff	H_r	0.005	0.06	[m]
	Soil saturation	H_{Gr3}	0.3	0.36	[m]
Cugnasco	Snow height	H_s	0	0.05	[m]
	Snow saturation	θ	0	0.1	[m]
	Runoff	H_r	0.004	0.05	[m]
	Soil saturation	H_{Gr3}	0.148	0.22	[m]
Sonogno	Snow height	H_s	0	0.05	[m]
	Snow saturation	θ	0	0.033	[m]
	Runoff	H_r	0.007	0.07	[m]
	Soil saturation	H_{Gr3}	0.17	0.24	[m]
Gima	Snow height	H_s	0	0.05	[m]
	Snow saturation	θ	0	0.017	[m]
	Runoff	H_r	0.007	0.07	[m]
	Soil saturation	H_{Gr3}	0.17	0.24	[m]
Rasiva	Snow height	H_s	0	0.05	[m]
	Snow saturation	θ	0	0.04	[m]
	Runoff	H_r	0.007	0.06	[m]
	Soil saturation	H_{Gr3}	0.17	0.23	[m]
Gerra	Snow height	H_s	0	0.03	[m]
	Snow saturation	θ	0	0.02	[m]
	Runoff	H_r	0.007	0.07	[m]
	Soil saturation	H_{Gr3}	0.17	0.24	[m]
Rovasch	Snow height	H_s	0	0.05	[m]
	Snow saturation	θ	0	0.03	[m]
	Runoff	H_r	0.006	0.06	[m]
	Soil saturation	H_{Gr3}	0.16	0.23	[m]

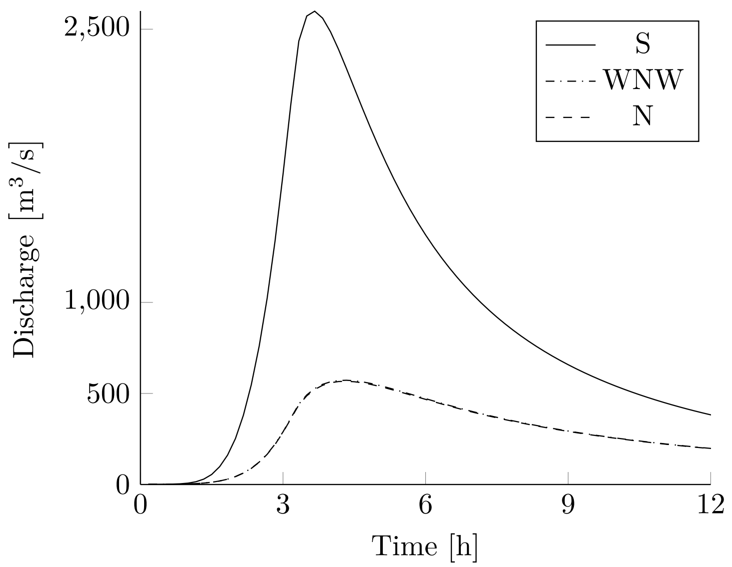

Figure 2.37: Hydrographs derived from 3h-PMPs for three different wind sectors: North (N), South (S) and West-North-West (WNW).

PMF estimates

After the determination of the most critical wind sector, the precipitation duration, generating the highest peak discharge has been determined. PMP durations from 1h to 10h have been simulated. The model has been initialized with the state variable values corresponding to the 99% quantile. The hourly averaged peak discharges are represented in Figure 2.38. It can be seen that the maximum hourly discharge of 4100 m^3/s has been generated by a 3h-PMP. The complete hydrographs, calculated with a time step of 10 minutes, are shown in Figure A.18. Comparing the peak discharge ($Q \approx 4200\,m^3/s$ for a 10 minutes time step) to the envelope curve of Marchi et al. (2010), described by the formula $Q_E = 97A^{0.6} = 2550\,m^3/s$, it can be stated that the ratio $\frac{Q}{Q_E} = 1.65$ would not lead to the conclusion of a significant overestimation of the PoMF. Such a verification is useful as the catchment is outside of the transition zone of the application limits of the Swiss PMP maps.

It has been retained that median initial conditions would be considered for the estimation of a safety flood. The critical PMP duration for the safety flood corresponds to the duration of the precipitation event that leads to the highest reservoir level. Figure 2.39 illustrates that the maximum reservoir level is reached for a PMP duration of 8h. The corresponding inflow and outflow hydrographs as well as the reservoir level evolution is shown in Figure 2.40. Thanks to the works undertaken to increase the spillway capacity of the Contra dam, described by Bremen and Bertola (1994), the 8h-PMP event combined with median initial conditions does not lead to overtopping. The hourly peak discharge corresponding to the safety flood has been estimated to be 2568 m^3/s. The return period of such a discharge has been estimated in section 2.3.7.

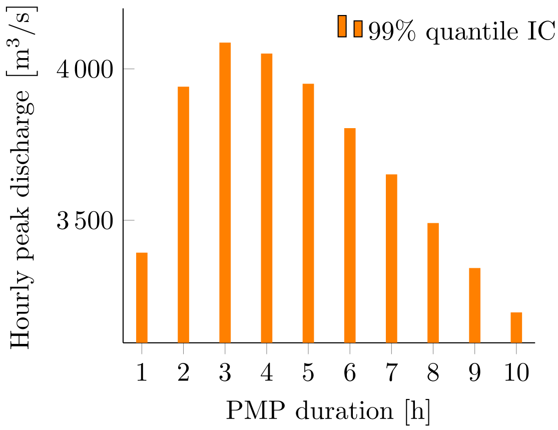

Figure 2.38: Hourly inflow peak discharges derived from different PMP events with wind sector "south" for the Contra dam catchment. "IC" stands for initial conditions.

2.3.7 Statistical extrapolation accounting for the estimated PMF

For this case study, hourly discharge data have been available. The discharge observation station Campioi-Lavertezzo (Figure 2.32) is situated inside the basin and measures the discharge generated by a catchment of $186 km^2$. This corresponds to 80% of the total catchment surface (A=$233 km^2$). It has been assumed that the flood discharges are proportional to the square root of the catchment area. The peak discharges observed at Campioi-Lavertezzo have been multiplied by $\sqrt{\frac{A_{tot}}{A_{CL}}} = 1.12$ ($A_{tot} = 233\ km^2$ is the total catchment area and $A_{CL} = 186\ km^2$ is the catchment area upstream of the Campioi-Lavertezzo observation station) to estimate the peak discharges at the outlet of the entire catchment.

The data set, used for the fit of the statistical distributions, is shown in Figure A.19. In the previous section, the hourly averaged PMF has been estimated to be 4100 m^3/s. This quantity has been considered as upper limit for the statistical extrapolation. The sample skewness of the yearly maximum discharge values has been estimated with Equation 2.2 to be $\gamma = 0.03$. This leads to the conclusion that, according to Takara and Tosa (1999), the LN4 distribution is most appropriate for the extrapolations. The fitted values using the LN4 distribution is shown in Figure 2.41. Furthermore, the more conventional GEV and log-normal distributions have been fitted. The POT method has been applied as well. A threshold of $u = 180\ m^3/s$ has been considered. This induces a data set, illustrated in Figure A.20, with 2.3 values per year. According to Tavares and Da Silva (1983), the average number of events per year should be around 2, in order to get the best performance of the POT method. Madsen (1996) concluded that good performances of the POT method can be awaited when the threshold definition results in 2 to 5 values per year. Figure 2.41 also shows the results of the three latter extrapolations. The estimated parameters for the different distribution are shown in appendix in Table A.6.

The statistical extrapolation using LN4, shown in Figure 2.41, has been used to attribute a return

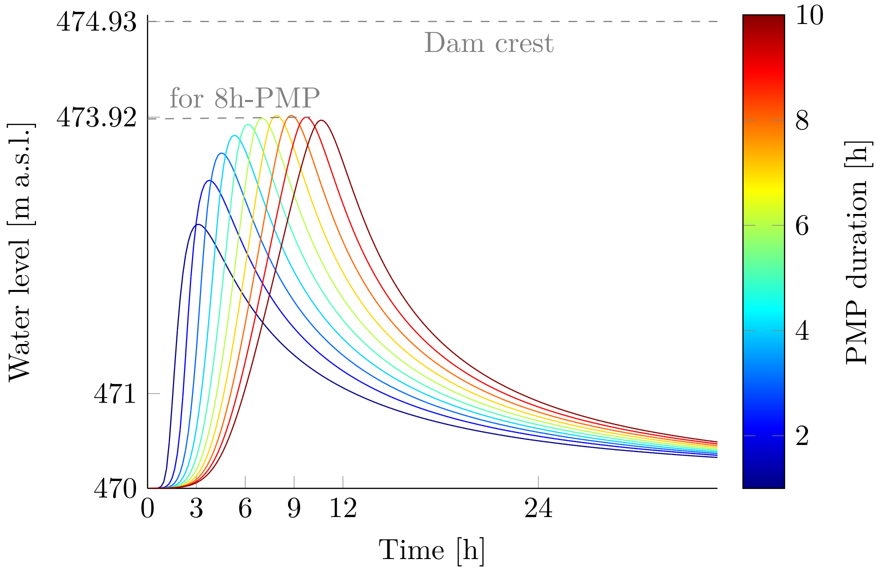

Figure 2.39: Contra dam reservoir level for different PMP events (wind sector "south") for 50% quantile initial values. The maximum level is reached for a 8h-PMP event.

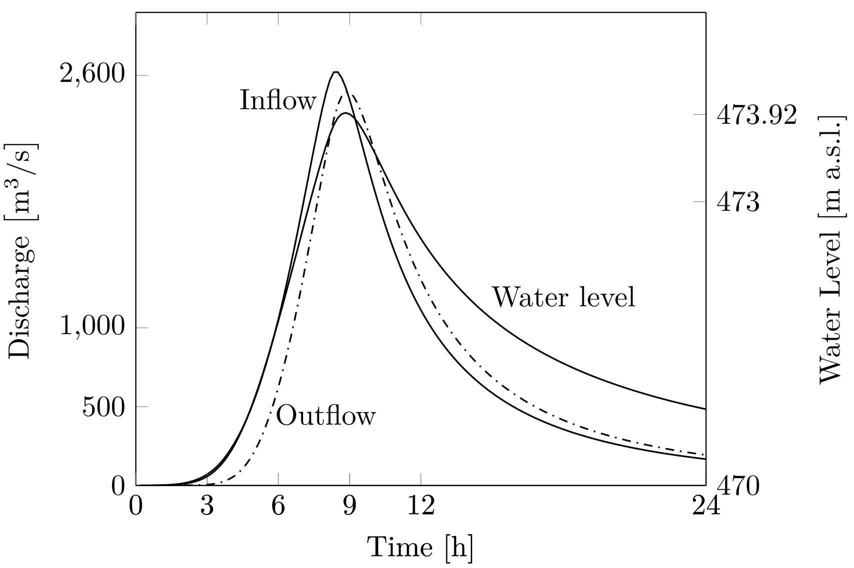

Figure 2.40: Inflow and outflow hydrographs with corresponding reservoir water level for a 8h-PMP event and median initial conditions.

period to the hourly averaged maximum discharge of the safety flood. The 8h-PMP combined with initial conditions being the median values of the state variable values, led to a discharge of 2568 m^3/s. The attributed return period is $1.7 \cdot 10^7$ years.

The LN4 distribution and POT method return the most similar extrapolations. The LN4 estimates are higher than the POT estimates for a certain return period. The log-normal distributions tends to overestimate the discharge for a certain return period compared to the LN4 distribution. The fact that the log-normal distribution reaches the PMF, assumed as upper limit, already for a return period of approximately 10^6 does not lead to much confidence in this extrapolation. In fact, the log-normal distribution overestimated the floods probably due to the fact that it only has two parameters. The fit of a two parameter distribution to a sample is only little influenced by larger values (DWA, 2012). The distribution is less flexible than a three parameter distribution and can thus in some cases not be fitted satisfactorily to the sample (DWA, 2012).

Regarding the GEV, the low skewness of the sample leads to a weibullian behaviour of the GEV ($\xi < 0$), meaning that it tends to a limit value. Therefore, compared to LN4 and POT, the GEV can be considered to underestimate the discharge estimates for high return periods.

According to the Swiss guidelines for dam safety (SFOE, 2008), the quantity $Q_s = 1.5Q_{1000}$ can be considered as safety flood. In this case, $Q_s = 2100$ m^3/s. The estimated discharge can be attributed a return period of slightly than $3 \cdot 10^5$ years according to the LN4 distribution. The safety flood derived under median initial conditions from the 8h-PMP has a peak discharge that is roughly 20% higher. Both estimations are close and coherent.

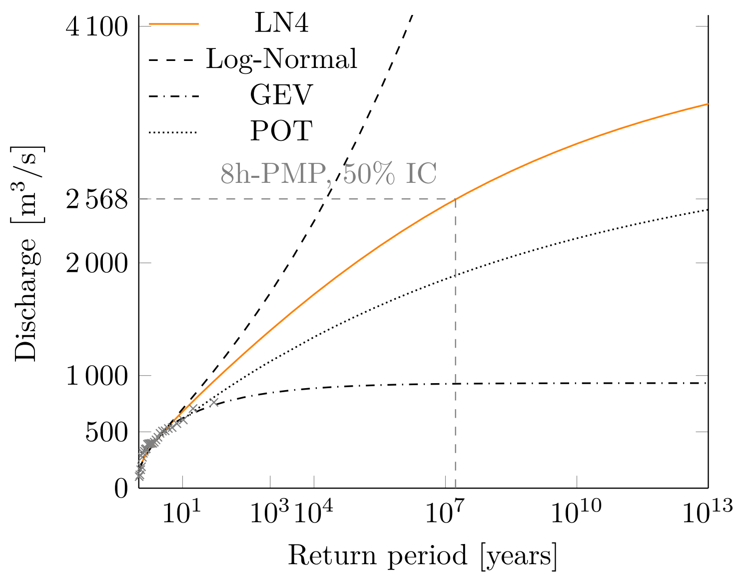

Figure 2.41: Annual maximum hourly discharge data fitted with the LN4 distribution considering an upper bound of PMF=4100m^3/s.

2.3.8 Intermediate conclusions

The case study of the Contra dam could show that the upper bounded statistical distribution LN4 gave more conservative estimates than the GEV and POT approach. The LN4 gave, however, smaller flood estimates than the log-normal distribution. The latter seems indeed not adapted for this case, as it has been mentioned earlier. The same conclusion can be drawn for the GEV, but for a different reason. The shape of the fitted distribution would simply not allow to attribute a reasonable return period to the PMF. thus the GEV does not seem adapted for the present case study, under the assumption that the PMF approach is valid.

The Contra dam catchment is slightly outside of the application limits for the CRUEX++ methodology (230 km^2). Therefore, an overestimation of the precipitation volume could have been occurring. Nevertheless, overtopping was not simulated for the considered safety flood. The outflow discharge, however, is larger than the spillway capacity given by SwissCOD (2011) (cf Table 2.5).

The return period estimated for the considered safety flood is $1.7 \cdot 10^7$ years. The return period of the quantity $Q_s = 1.5 Q_{1000}$ has also been estimated. It can be retained that the return period of $3 \cdot 10^7$ years would also fulfil the requirements of the Swiss dams safety guidelines (SFOE, 2008) that demand that the safety flood has to be much higher than the 1000 years.

3 Conclusions

The CRUEX++ methodology has been applied to three different dams. The catchments are differing in size, geographical situation and glacier cover. This allowed to apply the methodology to basins with different characteristics.

Comparing the results of the three case studies, i.e. Limmernboden, Mattmark and Contra, it can be concluded that the **return periods** estimated for the safety floods are **corresponding to the order of magnitude of the return periods associated to the PMF in literature**, i.e. 10^4 - 10^9 years (Cluckie and Pessoa, 1990; Resendiz-Carrillo and Lave, 1990; Shalaby, 1994; Smith, 1998; Hogg et al., 2004; Harris and Brunner, 2011; McClenathan, 2013). The range of these return periods is, however, very large. The uncertainty on its estimation is thus considerable. Generally, these return periods are estimated for PMF estimates that are assumed reasonable. It is normally not considered to be the possible maximum flood, but the probable maximum flood. The assumption of reasonable initial conditions (median state variable values) made for the applications led to return periods from 10^5 to 10^{11} years.

The largest return period has been determined for the case study of the Limmernboden dam. Different aspects let assume that the estimation of the safety flood having this return period is not exaggerated. A ratio of 1.3 between the simulated safety flood and $Q_s = 1.5Q_{1000}$ is reasonable. The uncertainty of Q_{1000}, in the case of Limmernboden, should be small in this case as all applied statistical distributions agreed on its estimation. Furthermore, the rather small slope of the extrapolation curve induces a considerable uncertainty on the estimate of the return period. Indeed, a small change of the discharge value leads to a large change of the related return period.

The advantage of the CRUEX++ methodology is that the combination of statistics and simulation form a holistic model that allows the estimation of the **discharge return periods and the hydrographs**. The eventual lack of extreme discharges in the observed time series induce conventional statistical approaches to over or underestimate the floods with a high return period. The **causal information expansion** performed in the CRUEX++ methodology allows to overcome this disadvantage. An example of this benefit can be illustrated by considering the extrapolation using the GEV and the log-normal distribution in the case of the Contra dam, discussed earlier.

In this application, the GEV could be identified to underestimate the flood discharges and the log-normal distribution was discussed to overestimate the latter. The CRUEX++ methodology allowed in this case to generate flood estimates in between the two doubtful extrapolations. Consequently, the credibility of the result could be significantly increased. It is perhaps not very dexterous to speak about credibility in the context of the Contra dam as it is situated outside of the application limits of the methodology. However, two things should be remembered. The catchment size is only slightly outside of the maximum admissible size and the determination of the upper area has been based on only 13 catchments, what induces a certain uncertainty on the estimated upper admissible catchment area. In the context of the argumentation on the extrapolation performed on the data of Contra, the sensitivity of the bounded extrapolation to the upper bound should not turn this conclusion in its contrary as the sensitivity of LN4 extrapolations to the estimation of the upper bound, are rather small.

Similar advantages could be found for the Limmernboden and Mattmark case study. In the case of the Limmernboden dam, the LN4 distribution could avoid underestimations from a return period of 10^3 years on. Especially the classical extreme value theory, postulating the usage of GEV and POT, was underestimating the flood discharges. The attribution of a return period to the safety flood was not even possible with these methods. The extrapolation to the simulated safety flood discharge would induce extremely high and unrealistic return periods, whereas the LN4 and log-normal distribution could show a similar behaviour and led to satisfactory results. For the case study of Mattmark, the extrapolation using the EV4 distribution could avoid to approach the deterministically estimated upper bound in an unrealistic manner as it could be observed and described for the GEV and POT method in section 2.2.6.

Finally, it can be concluded that the CRUEX++ methodology led to the most satisfactory results since unrealistic over and underestimations obtained by conventional statistical approaches could be overcome. **The combination of the statistics and the simulation based approach has the advantage to increase the plausibility of the results.**

Bibliography

Boillat, J. L. and Schleiss, A. (2000). *Création d'un volume de rétention supplémentaire dans la retenue de Mattmark pour la protection contre les crues*. Rapport N°4/00, Laboratoire de Constructions Hydrauliques (LCH). EPFL, Lausanne.

Boillat, J. L. and Schleiss, A. (2002). Détermination de la crue extrême pour les retenues alpines par une approche PMP-PMF. *Wasser Energie Luft*, 94(3/4):107–116.

Bremen, R. and Bertola, P. (1994). Increasing the spillway capacity of the Contra dam. *ICOLD Proceedings, XVIII Congress*, Q.68(R.27).

Cluckie, I. D. and Pessoa, M. L. (1990). Dam safety: an evaluation of some procedures for design flood estimation. *Hydrological Sciences Journal*, 35(5):547–569.

DWA (2012). *Merkblatt DWA-M 552. Ermittlung von Hochwasserwahrscheinlichkeiten*. DWA, Dt. Vereinigung für Wasserwirtschaft, Abwasser u. Abfall.

Harris, J. and Brunner, G. (2011). Approximating the probability of the probable maximum flood. *World Environmental and Water Resources Congress 2011, Proceedings*, pages 3695–3702.

Hertig, J.-A., Audouard, A., and Plancherel, A. (2005). Cartes des précipitations extrêmes pour la Suisse (PMP 2005). *Rapport EFLUM-EPFL.*

Hogg, W., Leytham, K., Neill, C., Sellars, C., and Watt, W. (2004). *Guidelines on extreme Flood Analysis*. Alberta Transportation, Transportation & Civil Engineering Division, Civil Projects Branch, Canada.

Jordan, F., Brauchli, T., Garcia Hernandez, J., Bieri, M., and Boillat, J. L. (2012). *RS 2012, Rainfall-Runoff Modelling. User guide*. unpublished manual. e-dric.ch, Lausanne.

KLL (1988). Kraftwerke Linth-Limmern AG, Stauanlage Limmernboden. Hochwasser Entlastung: Hydraulische Berechnung. Unpublished report. KLL Nr. 10988.

Madsen, H. (1996). *At-site and regional modelling of extreme hydrologic events*. PhD Thesis. Technical University of Denmark, Department of Hydrodynamics and Water Resources.

Marchi, L., Borga, M., Preciso, E., and Gaume, E. (2010). Characterisation of selected extreme flash floods in Europe and implications for flood risk management. *Journal of Hydrology*, 394(1–2):118–133.

McClenathan, J. T. (2013). We Can, But Should We? PMF Frequency Estimates. *World Environmental and Water Resources Congress 2013, Proceedings*, pages 1923–1928.

Moriasi, D. N., Arnold, J. G., Van Liew, M. W., Bingner, R. L., Harmel, R. D., and Veith, T. L. (2007). Model Evaluation Guidelines for Systematic Quantification of Accuracy in Watershed Simulations. *Transaction of ASABE*, 50(3):885–900.

Resendiz-Carrillo, D. and Lave, L. B. (1990). Evaluating Dam Safety Retrofits with Uncertain Benefits: The case study of Mohawk Dam (Walhonding River, Ohio). *Water Resources Research*, 26(5):1093–1098.

Schaefli, B., Hingray, B., Niggli, M., and Musy, A. (2005). A conceptual glacio-hydrological model for high mountainous catchments. *Hydrol. Earth Syst. Sci.*, 9(1/2):95–109.

Schaefli, B. and Zehe, E. (2009). Hydrological model performance and parameter estimation in the wavelet-domain. *Hydrol. Earth Syst. Sci.*, 13(10):1921–1936. HESS.

SFOE (2008). Sécurité des ouvrages d'accumulation. documentation de base relative à la véréfication de al sécurité en cas de crue. *Directives de l'OFEN*, Juin.

Shalaby, A. I. (1994). Estimating probable maximum flood probabilities1. *JAWRA Journal of the American Water Resources Association*, 30(2):307–318.

Smith, C. (1998). The PMF does have a frequency. *Canadian Water Resources Journal*, 23(1):1–7.

SwissCOD (2011). *Dams in Switzerland: Source for Worldwide Swiss Dam Engineering*. Swiss Commitee on Dams.

Takara, K. and Tosa, K. (1999). Storm and Flood Frequency Analysis using PMP/PMF Estimates. *Proceedings of International Symposium on Floods and Droughts, Nanjing, China, 18-20 October*.

Tavares, L. V. and Da Silva, J. E. (1983). Partial duration series method revisited. *Journal of Hydrology*, 64(1):1–14.

Appendix Part

A Methodology application

A.1 POT method

For the peak over threshold (POT) method, the Generalized Pareto distribution (GPD) is used. The expression of the cumulative density function and the probability density function are given by Equations A.1 and A.2 respectively.

$$F(x) = 1 - \left(1 + \xi \frac{x - s}{\sigma}\right)^{-1/\xi} \tag{A.1}$$

$$f(x) = \frac{1}{\sigma}\left(1 + \xi \frac{x - s}{\sigma}\right)^{-1/\xi - 1} \tag{A.2}$$

where $x > s$, s is the threshold and ξ is the shape parameter, σ the scale parameter.

The conversion of the quantiles into occurrence probabilities per year is explained in the following lines:

$n_o = \frac{n_d}{n_a}$ and $\zeta_s = \frac{n_s}{n_d}$

where n_d is the number of flood event data in the sample, n_a is the number of years, n_s the number of values above the threshold.

The Generalized Pareto distribution is fitted to the data above the chosen threshold. The quantiles corresponding to a certain return period T are then calculated by

$$x(T) = \begin{cases} s + \frac{\sigma}{\xi}\left[(T n_o \zeta_s)^{\xi} - 1\right] \;\; if \;\; \xi \neq 0 \\ s + \sigma \ln(T n_o \zeta_s) \;\; if \;\; \xi = 0 \end{cases}$$

A.2 Model performance coefficients

The Nash-Sutcliffe efficiency of defined by Equation A.3.

$$NS = 1 - \frac{\sum_{t=1}^{T}(Q_o^t - Q_s^t)^2}{\sum_{t=1}^{T}(Q_o^t - \overline{Q_o})^2} \tag{A.3}$$

where Q_o^t is the observed discharge at time t, Q_s^t is the simulated discharge at time t and $\overline{Q_o}$ is the mean observed discharge.

The Kling-Gupta efficiency is estimated by Equation A.4.

$$KGE = r^2(2\alpha - \alpha^2 - \beta^2) \tag{A.4}$$

where $r = \frac{\sum_{t=1}^{T}(Q_o^t - \overline{Q_o})(Q_s^t - \overline{Q_s})}{\sqrt{\sum_{t=1}^{T}(Q_o^t - \overline{Q_o})^2 \sum_{t=1}^{T}(Q_s^t - \overline{Q_s})^2}}$, $\alpha = \frac{\sum_{t=1}^{T}(Q_s^t - \overline{Q_s})^2}{\sum_{t=1}^{T}(Q_o^t - \overline{Q_o})}$ and $\beta = \frac{\overline{Q_s} - \overline{Q_o}}{\sum_{t=1}^{T}(Q_o^t - \overline{Q_o})}$. $\overline{Q_s}$ is the mean simulated discharge.

The volume ration is calculated with Equation A.5.

$$VR = \frac{V_s}{V_o} \tag{A.5}$$

Where V_s is the simulated volume and V_o the observed volume.

A.3 Application to the Limmernboden dam catchment

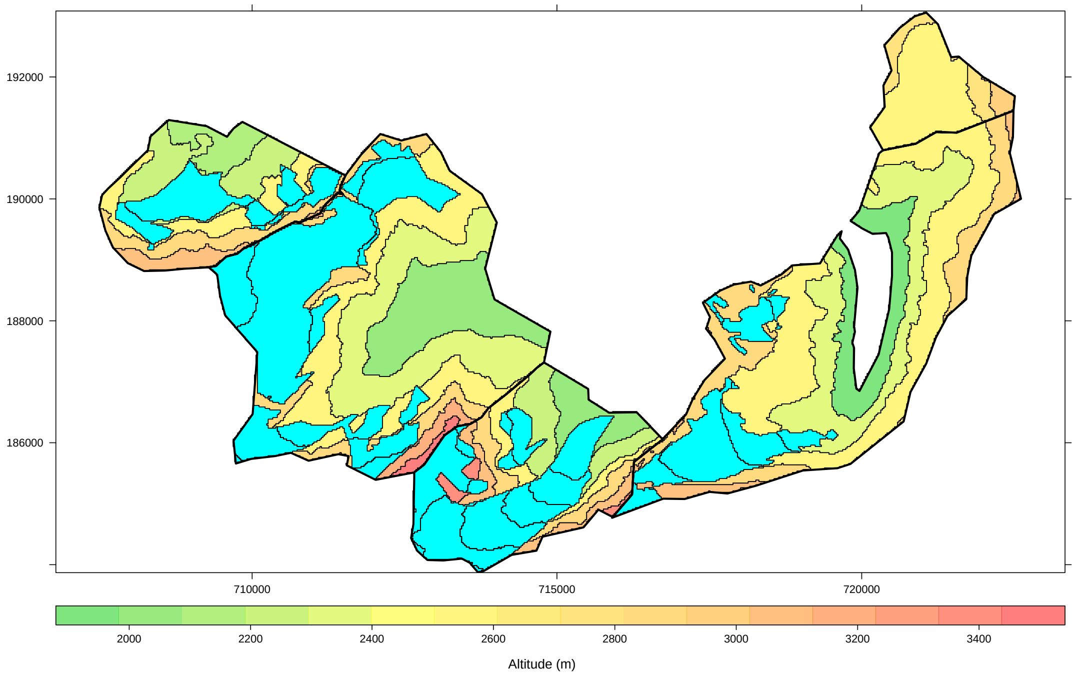

Figure A.1: Subdivision of the Limmernboden dam catchment in altitude bands with a vertical resolution of 300m. The glacier cover is shown in blue-green.

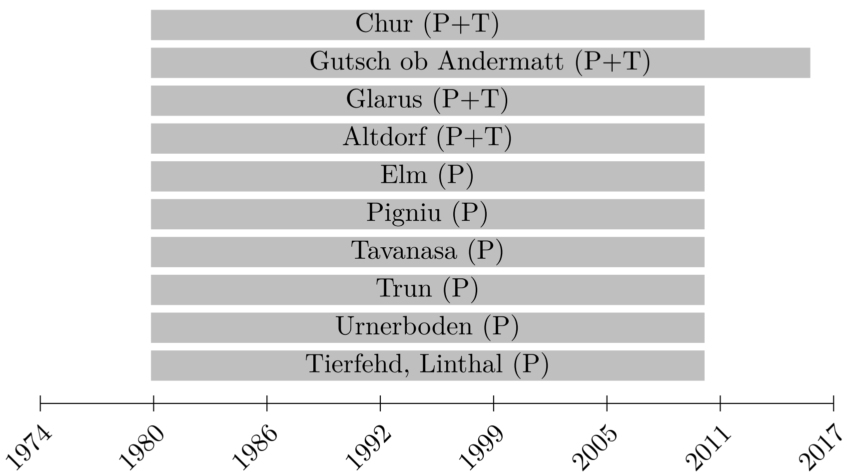

Figure A.2: Graphical data availability period representation for the meteorological stations considered for the calibration and validation for the *Limmernboden dam*.

Table A.1: Detailed dates per meteorological station, taken into account for the calibration and validation for the basin of the *Limmernboden dam*, with indication of the measured quantities.

Station	First value	Last value	Precipitation	Temperature
Tierfehd, Linthal	01.01.1980 00:00	31.12.2009 14:00	✓	
Urnerboden	01.01.1980 00:00	31.12.2009 14:00	✓	
Trun	01.01.1980 00:00	31.12.2009 17:00	✓	
Tavanasa	01.01.1980 00:00	31.12.2009 17:00	✓	
Pigniu	01.01.1980 00:00	31.12.2009 18:00	✓	
Elm	01.01.1980 00:00	31.12.2009 18:00	✓	
Altdorf	01.01.1980 00:00	31.12.2009 12:00	✓	✓
Glarus	01.01.1980 00:00	31.12.2009 11:00	✓	✓
Gutsch ob Andermatt	01.01.1980 00:00	24.09.2015 23:00	✓	✓
Chur	01.01.1980 00:00	31.12.2009 18:00	✓	✓

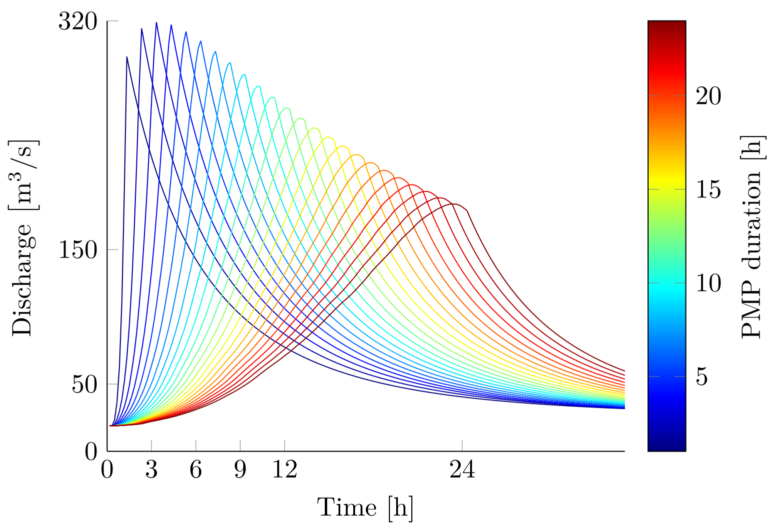

Figure A.3: Hydrograph estimates for the Limmernboden dam derived from different PMP events with wind sector "north". The simulation has been made with a 10 minutes time step and 99% quantile initial values.

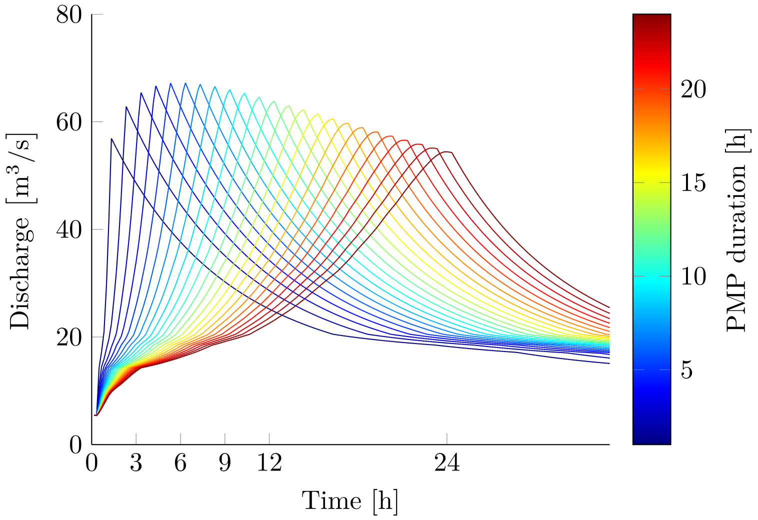

Figure A.4: Hydrograph estimates for the Limmernboden dam derived from different PMP events with wind sector "north". The simulation has been made with a 10 minutes time step and 50% quantile initial values.

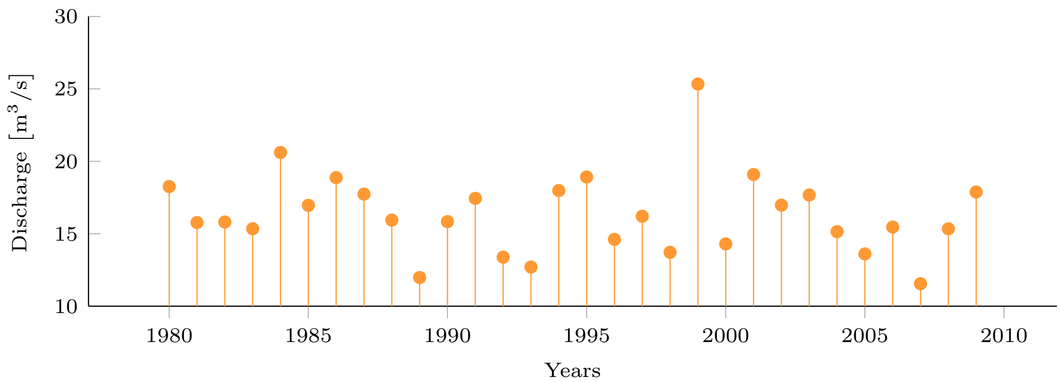

Figure A.5: Maximum annual discharges generated with the hydrological model with an hourly temporal resolution for the catchment of the Limmernboden dam.

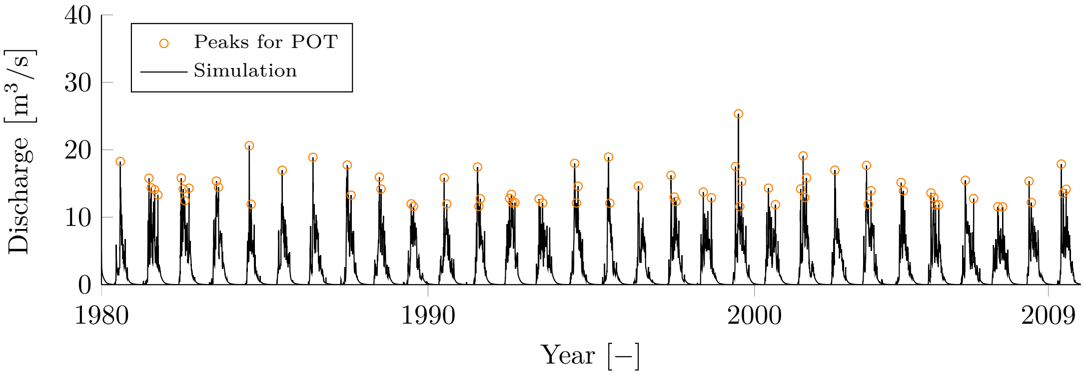

Figure A.6: Peak discharges over the threshold $u = 11.5\,\mathrm{m^3/s}$ generated with the hydrological model with an hourly temporal resolution for the catchment of the Limmernboden dam.

Table A.2: Parameters of the distribtuions estimated to fit the generated extremes for the Limmernboden dam. GP stands for General Pareto, the distribution used in the case of the POT method.

GEV	GP	log-normal	LN4
$\mu = 15.182$	$\sigma = 3.353$	$\mu = 2.781$	$\mu_Y = -2.775$
$\sigma = 2.362$	$\xi = -0.136$	$\sigma = 0.165$	$\sigma_Y = 0.173$
$\xi = -0.082$			$a = 0$

A.4 Application to the Mattmark dam catchment

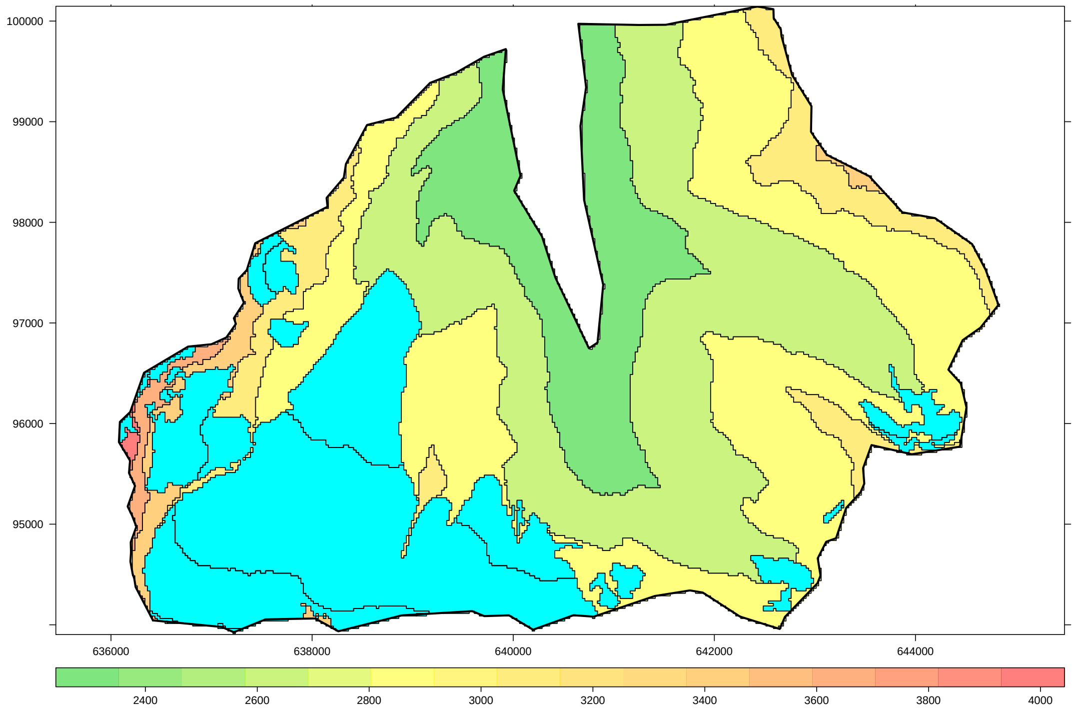

Figure A.7: Subdivision of the main Mattmark dam catchment in altitude bands with a vertical resolution of 300m. The glacier cover is shown in blue-green.

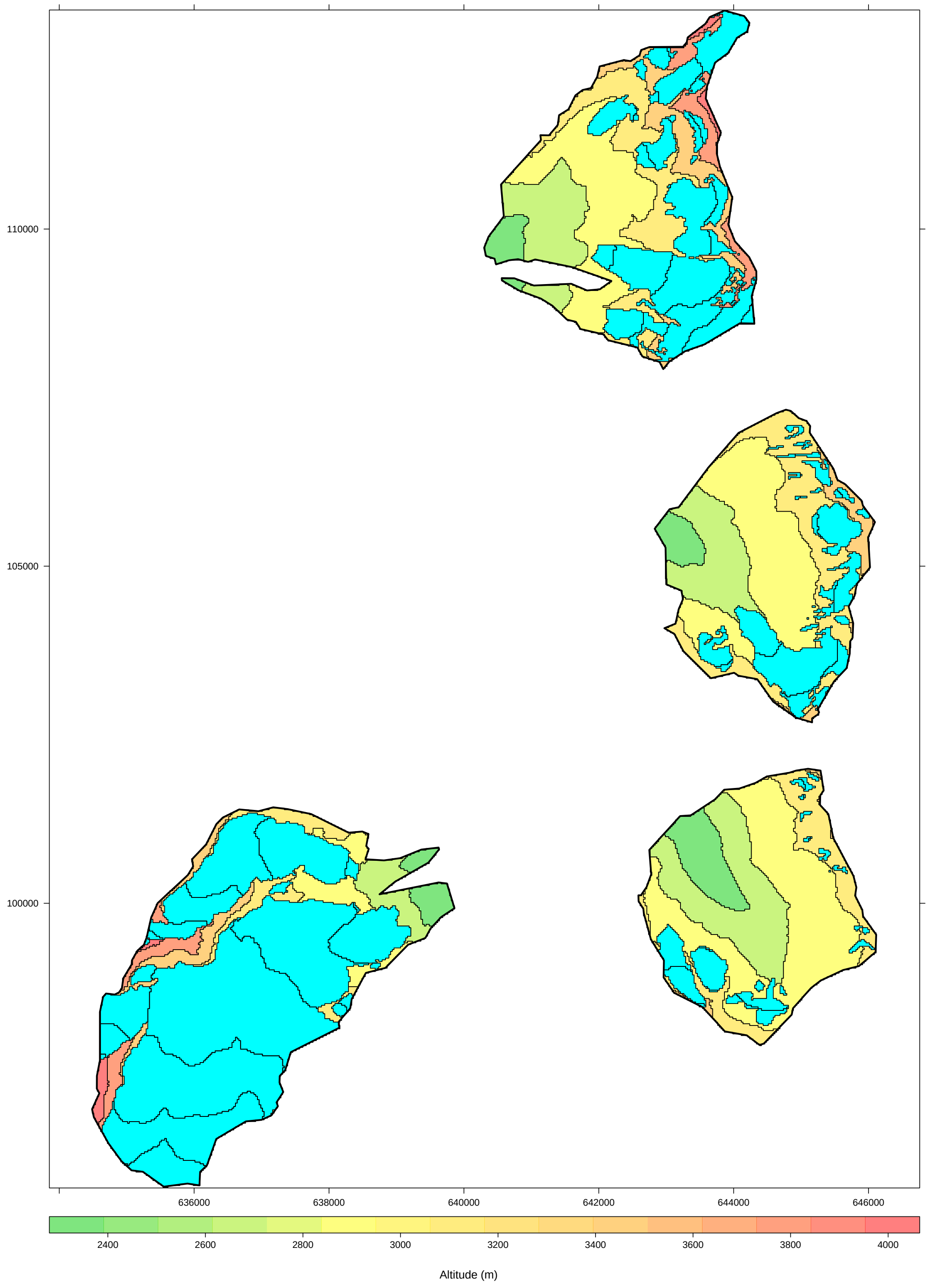

Figure A.8: Subdivision of the lateral Mattmark catchments in altitude bands with a vertical resolution of 300m. The glacier cover is shown in blue-green.

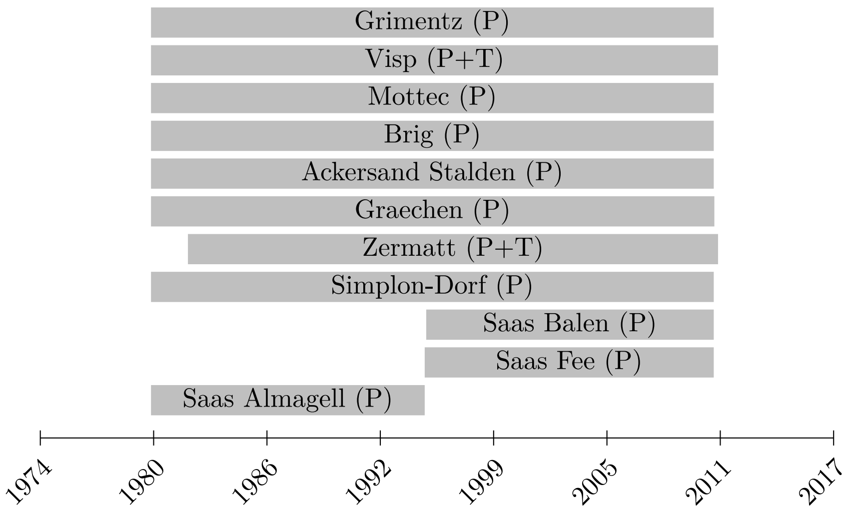

Figure A.9: Graphical data availability period representation for the meteorological stations considered for the calibration and validation for the *Mattmark dam*.

Table A.3: Detailed dates per meteorological station, taken into account for the calibration and validation for the basin of the *Mattmark dam*, with indication of the measured quantities.

Station	First value	Last value	Precipitation	Temperature
Saas Fee	01.11.1994 00:00	01.07.2010 06:00	✓	
Saas Balen	01.12.1994 00:00	01.07.2010 06:00	✓	
Saas Almagell	01.01.1980 00:00	01.09.1994 00:00	✓	
Simplon-Dorf	01.01.1980 00:00	01.07.2010 06:00	✓	
Zermatt	01.01.1982 00:00	24.09.2010 12:00	✓	✓
Graechen	01.01.1980 00:00	13.07.2010 06:00	✓	
Ackersand Stalden	01.01.1980 00:00	01.07.2010 06:00	✓	
Brig	01.01.1980 00:00	01.07.2010 06:00	✓	
Mottec	01.01.1980 00:00	01.07.2010 06:00	✓	
Visp	01.01.1980 00:00	24.09.2010 12:00	✓	✓
Grimentz	01.01.1980 00:00	01.07.2010 06:00	✓	

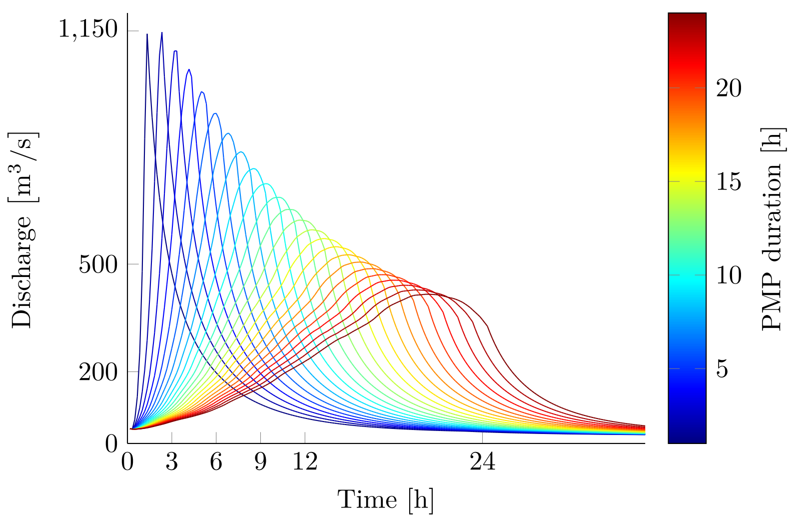

Figure A.10: Hydrographs derived from different PMP events with wind sector "south". The simulation has been made with a 10 minutes time step and 99% quantile initial values.

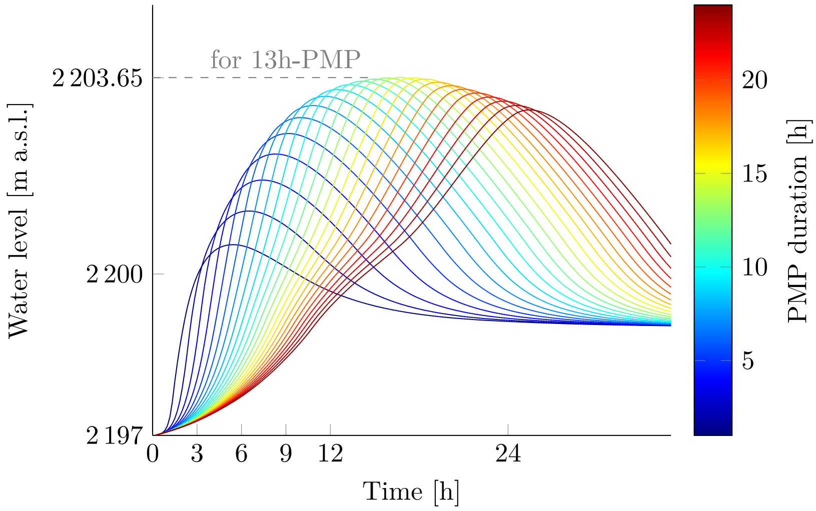

Figure A.11: Mattmark dam lake water level estimates for different PMP events (wind sector "south") for 99% quantile initial values. The maximum level is reached for a 13h-PMP event.

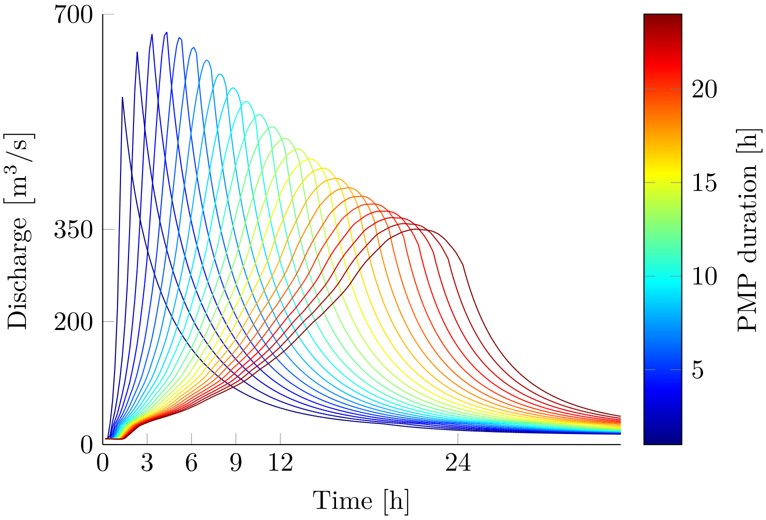

Figure A.12: Hydrographs derived from different PMP events with wind sector "south". The simulation has been made with a 10 minutes time step and 50% quantile initial values.

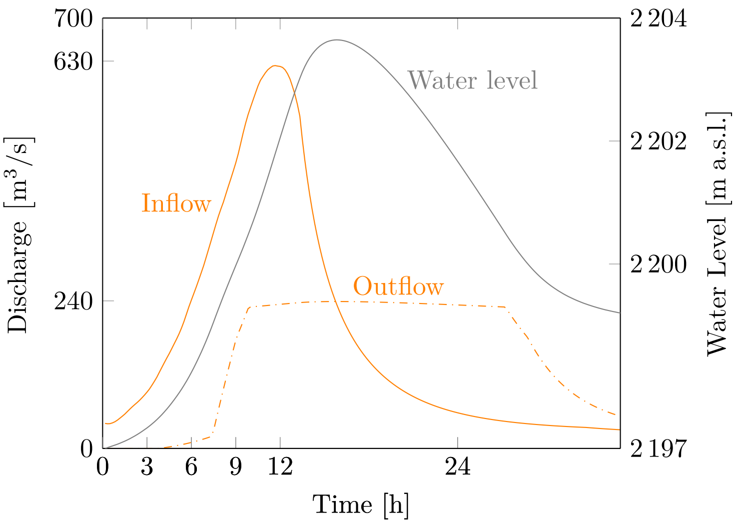

Figure A.13: Lake water level for different PMP events (wind sector "south") for 99% quantile initial values. The maximum level is reached for a 13h-PMP event.

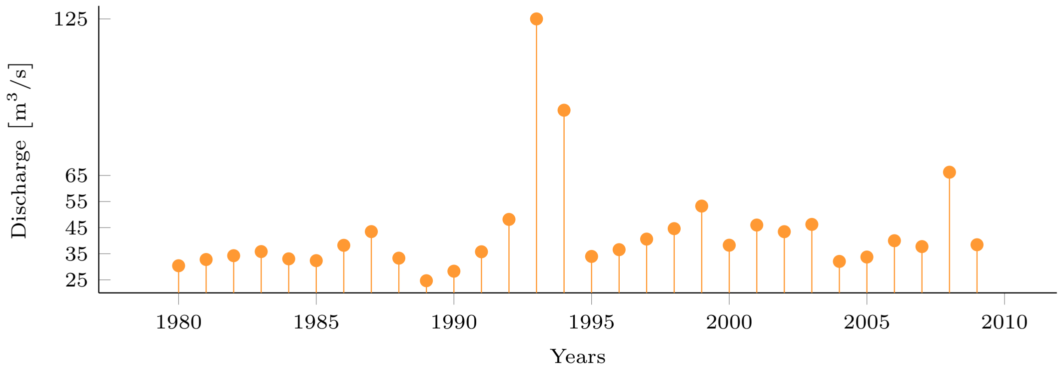

Figure A.14: Maximum annual discharge generated with the hydrological model with an hourly temporal resolution for the Mattmark dam.

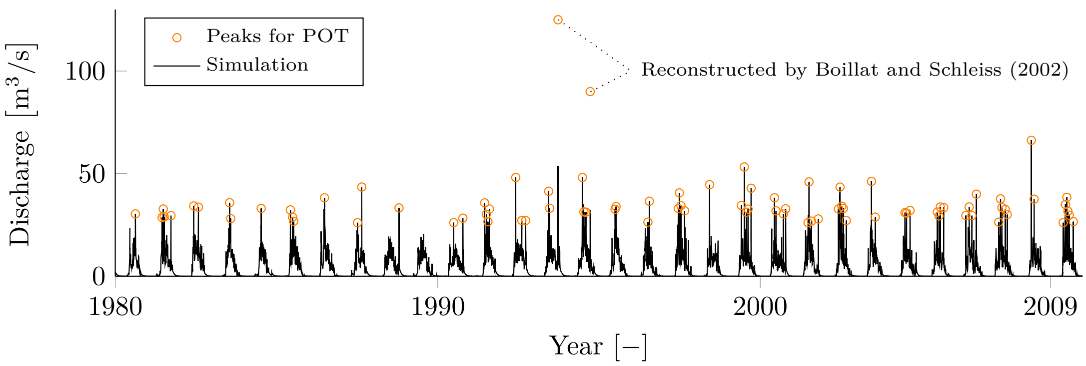

Figure A.15: Peak discharges over the threshold $u = 26\,\mathrm{m^3/s}$ generated with the hydrological model with an hourly temporal resolution for the catchment of the Mattmark dam.

Table A.4: Parameters of the distributions estimated to fit the generated extremes for the Mattmark dam. GP stands for Generalized Pareto, the distribution used in the case of the POT method.

GEV	GP	log-normal	EV4
$\mu = 35.24$	$\sigma = 7.741$	$\mu = 3.653$	$\nu = 36.87$
$\sigma = 7.712$	$\xi = 0.169$	$\sigma = 0.2096$	$k = 3.287$
$\xi = 0.283$			$a = 9.1$

A.5 Application to the Contra dam catchment

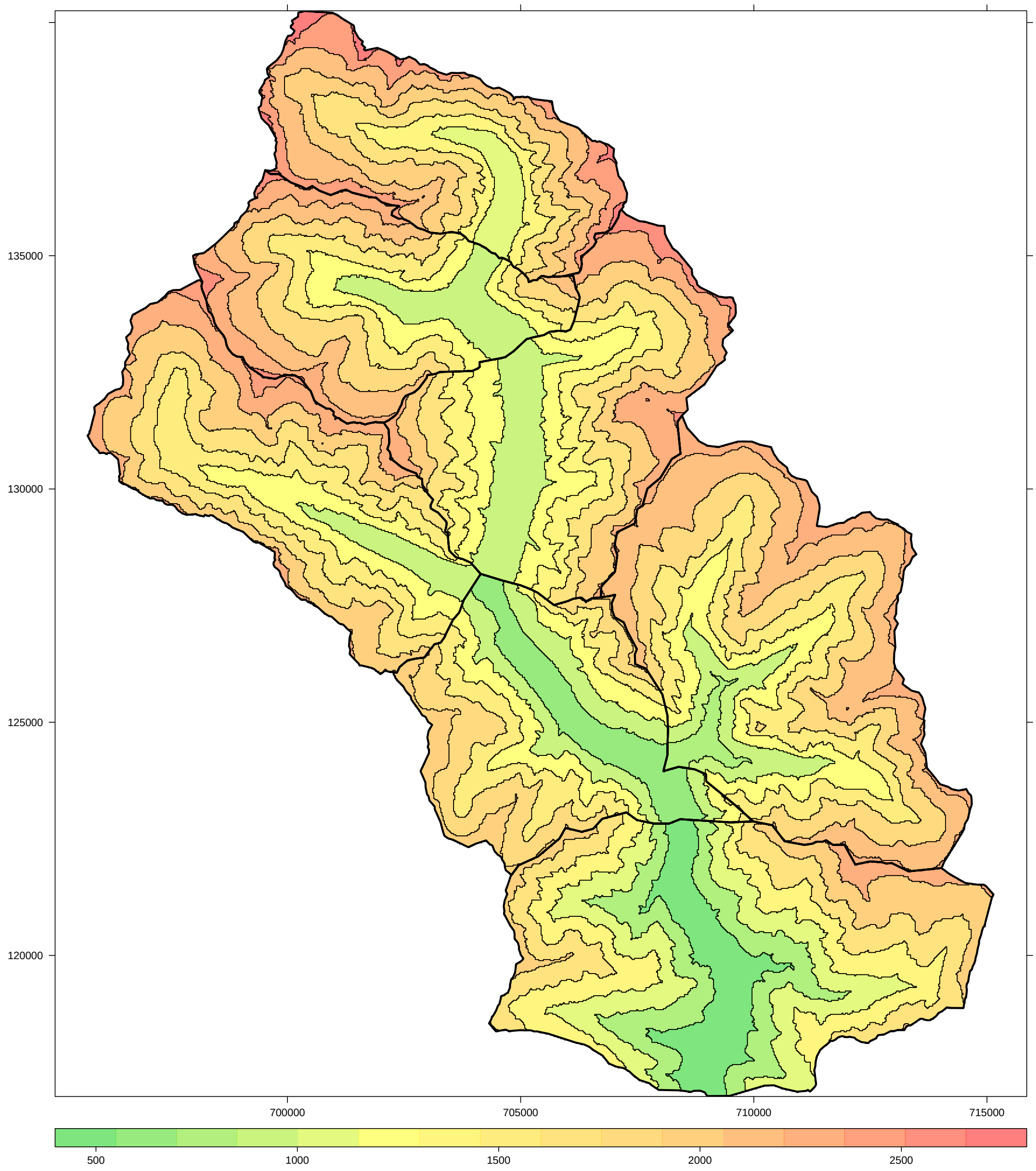

Figure A.16: Subdivision of the Contra dam catchment in altitude bands with a vertical resolution of 300m.

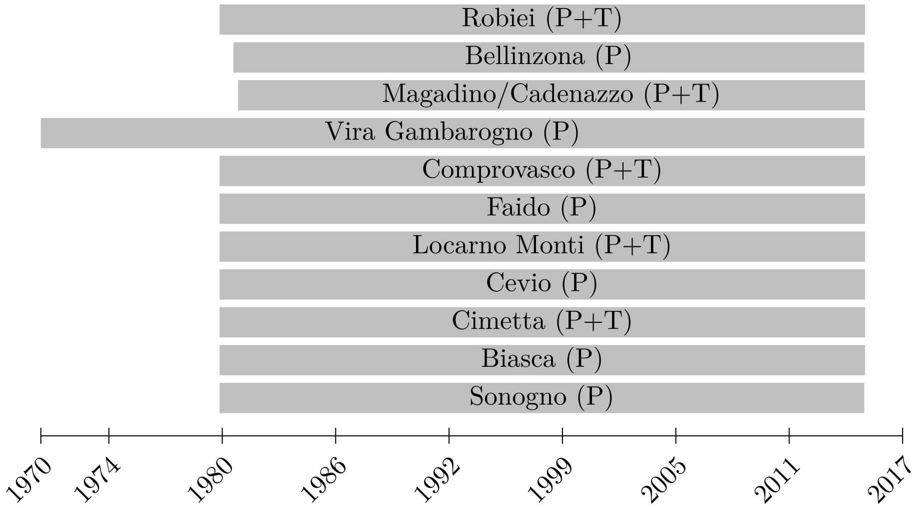

Figure A.17: Graphical data availability period representation for the meteorological stations considered for the calibration and validation for the *Contra dam*.

Table A.5: Detailed dates per meteorological station, taken into account for the calibration and validation for the basin of the *Contra dam*, with indication of the measured quantities.

Station	First value	Last value	Precipitation	Temperature
Sonogno	01.01.1980 00:00	01.12.2014 00:00	✓	
Biasca	01.01.1980 00:00	16.12.2014 00:00	✓	
Cimetta	01.01.1980 00:00	16.12.2014 12:00	✓	✓
Cevio	01.01.1980 00:00	16.12.2014 12:00	✓	
Locarno Monti	01.01.1980 00:00	16.12.2014 12:00	✓	✓
Faido	01.01.1980 00:00	16.12.2014 00:00	✓	
Comprovasco	01.01.1980 00:00	16.12.2014 12:00	✓	✓
Vira Gambarogno	01.01.1970 00:00	01.12.2014 00:00	✓	
Magadino/Cadenazzo	01.01.1981 00:00	16.12.2014 15:00	✓	✓

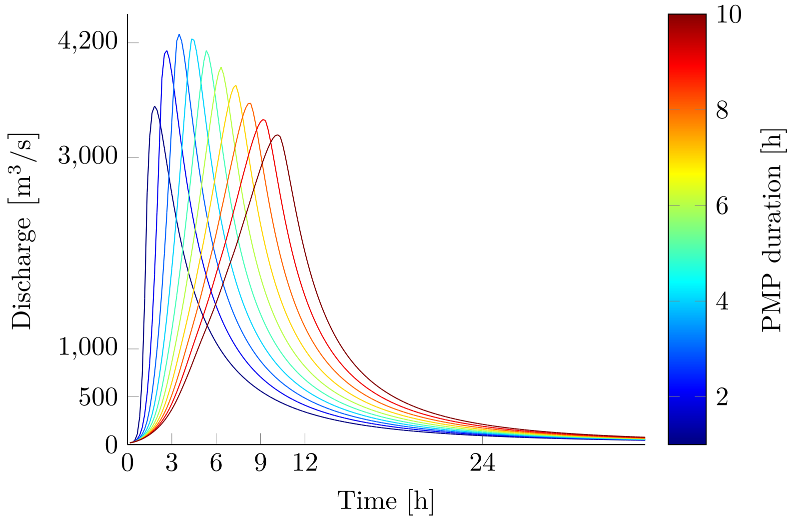

Figure A.18: Hydrographs derived from different PMP events with wind sector "south". The simulation has been made with a 10 minutes time step and 99% quantile initial values for the Contra dam catchment.

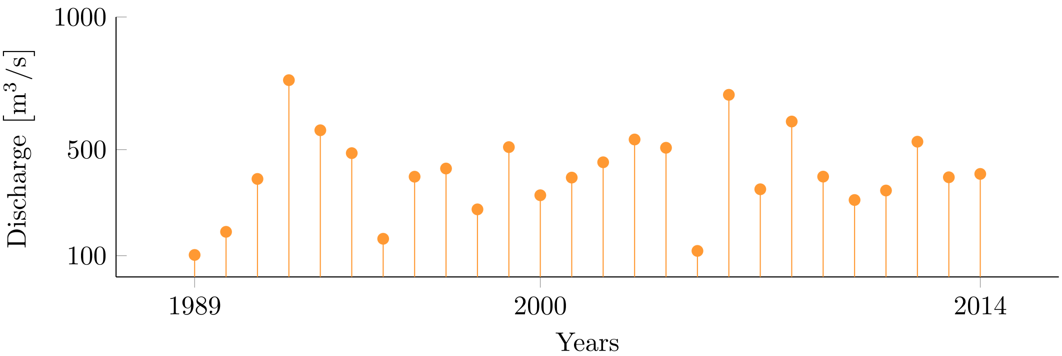

Figure A.19: Maximum annual discharge for the Contra dam catchment derived by scaling the discharges observed at the measurement station Campioi-Lavertezzo with a factor of $\sqrt{\frac{A_{tot}}{A_{CL}}} = 1.12$ ($A_{tot} = 233\ km^2$ is the total catchment area and $A_{CL} = 186\ km^2$ is the catchment area upstream of the Campioi-Lavertezzo observation station).

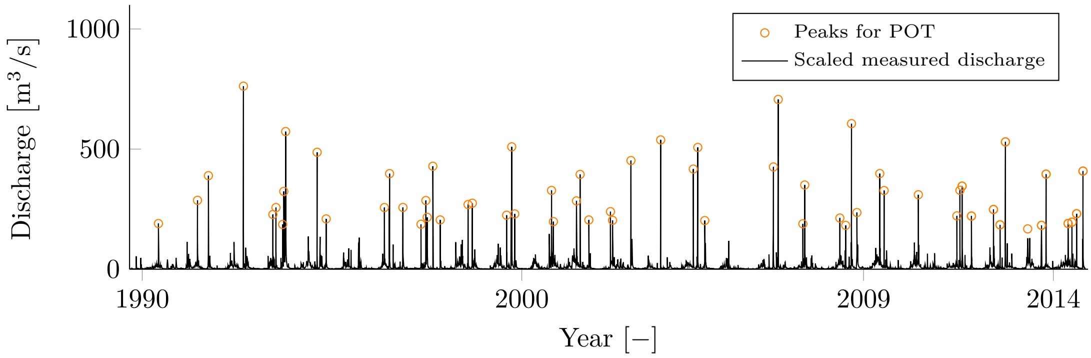

Figure A.20: Peak discharges over the threshold $u = 180\ \mathrm{m}^3/\mathrm{s}$ generated by scaling the discharges observed at the measurement station Campioi-Lavertezzo with a factor of $\sqrt{\frac{A_{tot}}{A_{CL}}} = 1.12$ ($A_{tot} = 233\ km^2$ is the total catchment area and $A_{CL} = 186\ km^2$ is the catchment area upstream of the Campioi-Lavertezzo observation station).

Table A.6: Parameters of the distributions estimated to fit the scaled observed extremes for the Contra dam. GP stands for Generalized Pareto, the distribution used in the case of the POT method.

GEV	GP	log-normal	LN4
$\mu = 353.34$	$\sigma = 147.812$	$\mu = 5.917$	$\mu_Y = -2.295$
$\sigma = 159.91$	$\xi = -0.0511$	$\sigma = 0.498$	$\sigma_Y = 0.530$
$\xi = -0.276$			$a = 0$